RADC-TR-71-236
Final Technical Report
March 1971

Prepared By
Rome Air Development Center
Air Force Systems Command
Griffiss Air Force Base, New York 13440

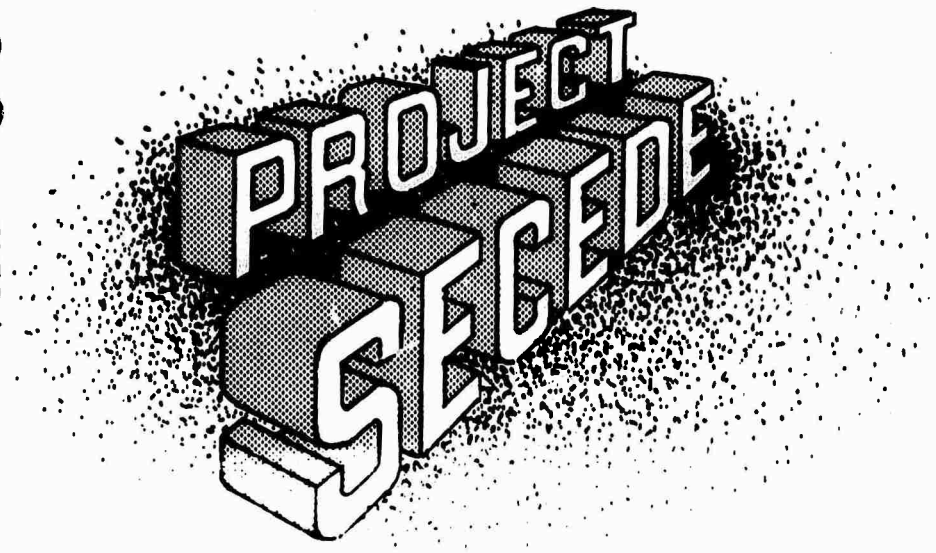

OPERATION OF THE SECEDE II LOBE-SWEEP INTERFEROMETERS

Northwest Environmental Technology Laboratories, Incorp.

Sponsored by
Advanced Research Projects Agency
ARPA Order No. 1057

51

UNCLASSIFIED

Security Classification

DOCUMENT CONTROL DATA - R & D

(Security classification of title, body of abstract and indexing annotation must be entered when the overall report is classified)

1 ORIGINATING ACTIVITY *(Corporate author)*
Northwest Environmental Technology Labs.
Bellevue, WA 98005

2a. REPORT SECURITY CLASSIFICATION
UNCLASSIFIED

2b. GROUP

3 REPORT TITLE
Operation of The SECEDE II Lobe-Sweep Interferometers

4 DESCRIPTIVE NOTES *(Type of report and inclusive dates)*
Final Report

5. AUTHOR(S) *(First name, middle initial, last name)*
John M. Lansinger
Maurice H. Evans, Jr.

6. REPORT DATE	7a. TOTAL NO OF PAGES	7b. NO OF REFS
March 1971	55	

8a. CONTRACT OR GRANT NO.	9a. ORIGINATOR'S REPORT NUMBER(S)
F30602-71-C-0023	NETL-2
b. PROJECT NO. ARPA Order Nr. 1057	
c. Program Code Nr. 0E20	9b. OTHER REPORT NO(S) *(Any other numbers that may be assigne this report)*
d.	RADC-TR-71-236

10 DISTRIBUTION STATEMENT
Approved for public release; distribution unlimited.

11. SUPPLEMENTARY NOTES	12. SPONSORING MILITARY ACTIVITY
Monitored by: RICHARD W. CARMAN RADC/OCSE Griffiss AFB NY 13440	Advanced Research Projects Agenc 1400 Wilson Blvd Arlington VA 22209

13. ABSTRACT

Two pairs of twin-element, lobe-sweep radio interferometers have been designed, constructed, bench-tested and operated in the field during the SECEDE II test series. One pair operates at a frequency of 145.7644 MHz, the other at 437.2932 MHz. The total of four interferometers is realized with three circularly polarized, broadband log-periodic antennas spaced equally along a two-hundred-meter baseline with the center antenna common to each interferometer pair. Recorded interferometer outputs at each frequency include (1) a quasi-logarithmic signal amplitude from each antenna; (2) two phase difference measurements between antenna pairs of each interferometer, one direct, and the other shifted in phase by π radians; and (3) a differential phase measurement, i.e., the difference between the individual interferometer phase difference measurements. Generated block diagrams of the interferometer systems are presented, as are results of the bench tests of system performance.

DD FORM 1 NOV 65 1473

UNCLASSIFIED

Security Classification

When US Government drawings, specifications, or other data are used for any purpose other than a definitely related government procurement operation, the government thereby incurs no responsibility nor any obligation whatsoever; and the fact that the government may have formulated, furnished, or in any way supplied the said drawings, specifications, or other data is not to be regarded, by implication or otherwise, as in any manner licensing the holder or any other person or corporation, or conveying any rights or permission to manufacture, use, or sell any patented invention that may in any way be related thereto.

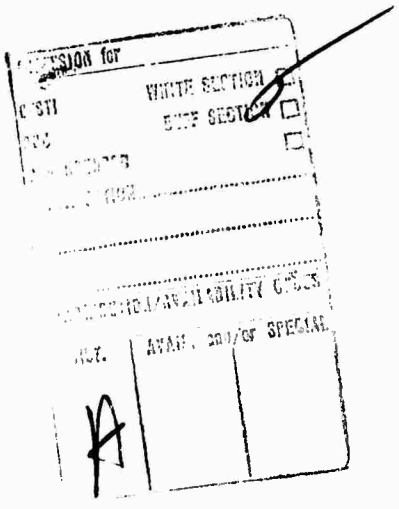

If this copy is not needed, return to RADC (OCSE), GAFB, NY 13440.

14 KEY WORDS	LINK A		LINK B		LINK C	
	ROLE	WT	ROLE	WT	ROLE	WT
Radio Interferometer						
Radio-frequency Beacons						

ABSTRACT

Two pairs of twin-element, lobe-sweep radio interferometers have been designed, constructed, bench-tested and operated in the field during the SECEDE II test series. One pair operates at a frequency of 145.7644 MHz, the other at 437.2932 MHz. The total of four interferometers is realized with three circularly polarized, broadband log-periodic antennas spaced equally along a two-hundred-meter baseline with the center antenna common to each interferometer pair. Recorded interferometer outputs at each frequency include (1) a quasi-logarithmic signal amplitude from each antenna; (2) two phase difference measurements between antenna pairs of each interferometer, one direct, and the other shifted in phase by π radians; and (3) a differential phase measurement, i.e., the difference between the individual interferometer phase difference measurements. A description is given of the overall instrumentation and its operation.

OPERATION OF THE SECEDE II LOBE-SWEEP INTERFEROMETERS

J. M. Lansinger
M. H. Evans, Jr.

Contractor: Northwest Environment Technology Laboratories, Incorporated
Contract Number: F30602-71-C-0023
Effective Date of Contract: 14 August 1970
Contract Expiration Date: 31 March 1971
Amount of Contract: $119,732.00
Program Code Number: 0E20

Principal Investigator: John M. Lansinger
Phone: 206 455-3510

Project Engineer: Vincent J. Coyne
Phone: 315 330-3107

Contract Engineer: Richard Carman
Phone: 315 330-2478

This research was supported by the Advanced Research Projects Agency of the Department of Defense and was monitored by Richard Carman RADC (OCSE), GAFB, NY 13440 under contract F30602-71-C-0023.

FORWARD

This is technical report number 2 covering the period 1 December 1970 to 31 January 1971 on Northwest Environmental Technology Laboratories project 70-001.

Approved for publication

for Northwest Environmental Technology Laboratories:

William T. Kreiss
Director of Research

William G. Tank
Director of Technical Services

for Rome Air Development Center:

Vincent J. Coyne
Project Engineer

Richard W. Carman
Contract Engineer

CONTENTS

FIGURES

TABLES

BLANK PAGE

I. INTRODUCTION

The SECEDE II transmission experiment review committee, 6 December 1969, recommended that interferometer measurements be implemented in the SECEDE II RF beacon ground measurements. Information about the structure and ion content of barium clouds produced during this test series was to be obtained principally from the dispersive phase measurements. The primary purpose of the interferometer data was to indicate the relative importance of diffraction in the interpretation of the dispersive phase data.

An interim report has been prepared and distributed (Ref. 1) in which the basic interferometer design was described, and the results of the bench acceptance test reported. A catalog of the data obtained in the field, and a summary of the interferometer SECEDE II data reduction procedures has been presented in a special report. The purpose of this final report is to describe in detail the lobe-sweep instrumentation, and to present relevant information previously unreported relating to the operation and testing of the equipment.

II. DESCRIPTION OF THE EQUIPMENT

A. GENERAL REQUIREMENTS

Two pairs of twin-element, lobe-sweep radio interferometers were designed for the SECEDE II transmission experiments. One pair operated at a frequency of 145.7644 MHz, the other at 437.2932 MHz. The total of four interferometers was realized with three circularly polarized, broadband log-periodic antennas spaced equally along a two-hundred-meter baseline, with the center antenna common to each interferometer pair.

The interferometer outputs at each frequency consisted of the following:

1. A quasi-logarithmic amplitude output was obtained from each antenna.

2. Two measures of the phase difference between antenna pairs of each interferometer were provided, one direct, the other shifted in phase

by π radians. The latter output was provided to ensure a complete record of phase fluctuations uncontaminated by step transitions.

3. For each pair of interferometers an on-line measurement was made of the difference in phase outputs between adjacent antenna pairs. This measurement is referred to as the second difference in phase. A spatial phase gradient in the incident wavefront large compared to the total antenna separation resulted in nearly equal outputs from adjacent antenna pairs; consequently, the second difference in phase was in this instance minimal. On the other hand, variations in wave tilt of a scale comparable to the antenna separation resulted in an appreciable output in the second difference in phase.

B. BASIC OPERATING PRINCIPLE

The operating principle of the lobe-sweep interferometer is outlined by the block diagram of the basic system shown in figure 1. As indicated by the figure, an incoming signal at a frequency f_{rf} is received by antennas A_1 and A_2. Given a plane wave with an incident angle θ_i as shown in the figure, the electrical phase difference of the received signal is:

$$\phi = \frac{2\pi D\, f_{rf}\, \mathrm{Sin}\,(\theta_i)}{c} \qquad (1)$$

where D is the antenna separation and c is the velocity of propagation.

As indicated by the figure, the two local oscillator signal inputs to the mixers are offset by the reference clock frequency Δf. The clock frequency is chosen to be low compared to the over-all receiver bandwidth, but high compared to the highest phase frequency which was to be measured by the system. The intermediate frequency f_{if} coming from the two antenna signal sources is offset by the clock frequency Δ_f (figure 1). Subsequent addition of the two signals, detection and low-pass filtering resulted in a signal component given by:

$$K_3\, A_1 A_2\, \mathrm{Sin}\,[(\Delta f)t + \theta(t) + \gamma] \qquad (2)$$

The factor K_3 takes into account conversion factors and gain constants through the system. The phase factor γ is a phase angle to account for phase shifts internal to the instrumentation system, i.e., differential antenna cable lengths, etc.

The output of the phase meter shown in figure 1 provides a measure of the difference in phase between the two input signals. Thus, the time varying output $\phi(t)$ from the phase meter can be interpreted as a variation in the incident angle $\theta(t)$ in accordance with equation (1). In practice the measured quantity ϕ has a peak-to-peak range of 2π radians before repeating itself. There is therefore an ambiguity of $2\pi N$ in the measurement of $\phi(t)$. This ambiguity is resolved utilizing trajectory information which allows the determination of the incident angle of the beacon signal with respect to the interferometer baseline.

During the period when the beacon was tracked by the system, the factor $\phi(t)$ varied with time due to both the motion of the beacon and to the presence of ionization gradients within the barium cloud. At the time of occultation, the phase variations caused by such ionization gradients were of primary interest. It was therefore necessary to remove from the data the phase variations due to the motion of the beacon. The procedure for removing such variations is relatively straight-forward and has been discussed in a previous report (Ref. 2).

C. DETAILED SPECIFICATIONS

Table 1 lists the system requirements which were satisfied for the lobe-sweep interferometer operated during the SECEDE II test series. The bench test set-up procedure, together with the acceptance test results, have been published in a previous report (Ref. 1).

The beacon acquisition time at both frequencies was within 2 seconds of the beacon launch. The specification for amplitude and phase difference measurement was compatible with a beacon having a minimum ERP of -6dbw at 145.7644 MHz and -3dbw at 437.2932 MHz. For the SECEDE II operations the beacon signal polarization was linear along the rocket axis. Antenna pattern measurements and determination of minimum signal input levels have been published in a previous report (Ref. 1).

SPECIFICATION	FREQUENCY			
	145.7644 MHz		437.2932 MHz	
Error in recovered phase difference due to noise and receiver and recording instabilities	<0.04 <0.2	rad rms rad peak	<0.04 <0.2	rad rms rad peak
Averaging time for receiver instabilities	>70	s	>70	s
Deviation from mean signal voltage (that for free space propagation) due to noise and receiver and recording instabilities	<0.5 <1.2	db rms db peak	<0.5 <1.2	db rms db peak
Margin for instantaneous peak signal over mean level	>20	db	>20	db
3 db cutoff frequency of amplitude and phase measurement	>150	Hz	>60	Hz
Deviation in phase difference with ±20 db variation in input signal level	<0.03	rad rms	<0.03	rad rms
3 db IF bandwidth	>300	Hz	>120	Hz
Doppler shift tolerance from rocket motions	>1	KHz	>3	KHz
Minimum range	100	km	100	km
Maximum range	600	km	600	km

The interferometer receiving antennas at both frequencies satisfy the following specifications:

Polarization	Circular	
Rejection of opposite circular polarization	>20 >10	db on bore sight db within half power beam
3 db azimuthal coverage	>65°	
3 db elevation coverage	10-75°	

TABLE I - SUMMARY OF SPECIFICATIONS - LOBE-SWEEP INTERFEROMETER

D. SYSTEM DETAILS - GENERAL

The equipment essentials are summarized in the simplified block diagram of figure 2. More complete details are given in figures 3 and 4. The interferometer antennas were mounted approximately forty feet above the ground on remotely controlled elevation-azimuth rotators on poles which were equally spaced along a two-hundred-meter baseline. During data acquisition, the antennas remained fixed in position for the period that the signal from the beacon was monitored. Preamplifiers were mounted on the poles in proximity to each antenna to minimize system noise figures. Two calibration monopole antennas, one for each frequency, were mounted on a fourth pole removed from the interferometer antenna array. All other equipment for signal processing, recording and calibration were housed in a trailer central to the receiving antennas.

As indicated in figure 2, the signal received by the antennas is amplified by low noise preamplifiers, converted to 30 MHz, and further amplified. Narrow-band, crystal filters are used in the 30 MHz amplifier to limit the predetection noise bandwidth, while still providing adequate bandwidth to accommodate expected Doppler shifts in beacon signals.

The quasi-logarithmic amplitude outputs are taken for recording from the AGC signal controlling the gain of the 30 MHz amplifiers. The dynamic response of the amplitude output is determined by the slope of the AGC voltage versus the IF amplifier gain curves.

The two local oscillator signal inputs to the mixers are offset by the 3 KHz clock frequency. A beacon signal received by the antennas therefore resulted in a 3 KHz output signal from the detector shown in figure 2. The output of the phase meter is linearly related to the phase difference between the clock and signal inputs to it, and thus provides a measure of the path difference of the beacon signal between receiving antennas.

A summary of the recording instrumentation and recorded parameters is presented in Table II. The purpose of the strip chart recording was to provide back-up data and on-line visual data for quick-look analysis. The magnetic recordings were obtained in accordance with a standard fm-IRIG format at 15 ips. Subsequent analysis involved digitizing the fm analog tapes and processing the results by computer.

PRECISION INSTRUMENTS
MAGNETIC TAPE RECORDING
(one-inch)

Track - 1	A1 LF
Track - 2	A2 LF
Track - 3	A3 LF
Track - 4	$\phi_{3,2}$ LF
Track - 5	$\phi_{1,2}$ LF
Track - 6	$\phi_{3,2}$ (π) LF
Track - 7	$\phi_{1,2}$ (π) LF
Track - 8	A1 HF
Track - 9	A2 HF
Track - 10	A3 HF
Track - 11	$\phi_{3,2}$ HF
Track - 12	$\phi_{1,2}$ HF
Track - 13	$\phi_{3,2}$ HF
Track - 14	IRIG B TIME

AMPEX MAGNETIC TAPE RECORDING
(one-half-inch)

Track - 1	IRIG B TIME
Track - 2	$\phi_{1,2}$ (π) HF
Track - 3	2nd Difference Phase LF
Track - 4	2nd Difference Phase HF

TECHNI-RITE STRIP CHART RECORDING

Chan. - 1	A1 LF
Chan. - 2	A2 LF
Chan. - 3	$\phi_{3,2}$ LF
Chan. - 4	2nd Difference Phase LF
Chan. - 5	A1 HF
Chan. - 6	A2 HF
Chan. - 7	$\phi_{3,2}$ HF
Chan. - 8	2nd Difference Phase HF

A1	element amplitude northern antenna
A2	element amplitude middle antenna
A3	element amplitude southern antenna
$\phi_{1,2}$	phase difference between elements 1 and 2
$\phi_{3,2}$	phase difference between elements 3 and 2
π	indicates phase ambiguity channel
LF	measurements at 145.7644 MHz
HF	measurements at 437.2932 MHz

TABLE II - SUMMARY OF RECORDING INSTRUMENTATION AND RECORDED PARAMETERS

1. RF System

The rf portion of the instrumentation is summarized in the block diagram shown in figure 3. The antennas are log-periodic dipole antenna assemblies which provide 8 db gain relative to a circularly polarized source. The right and left-handed circularly polarized outputs from the antenna assemblies are fed into 145 MHz and 437 MHz interferometer systems, respectively. The preamplifier housing units shown in detail in figure 4 were mounted in close proximity to the antennas to minimize loss, thereby minimizing the over-all system noise figure. At the 437 MHz center frequency, the maximum noise figure of the preamplifiers was 3.5 db, the minimum 3 db bandwidth was 10 MHz, and the minimum gain was 30 db. At the 145 MHz center frequency, the comparable preamplifier specification figures were 2.9 db, 10 MHz, and 30 db, respectively.

The rf signals following preamplification were fed via low-loss cables to a central trailer where the remainder of the signal processing was carried out. The rf signals were converted to the 30 MHz intermediate frequency in the mixer-amplifier-filter units shown in detail in figure 5. As shown in the figure, a double-balanced mixer was employed. The mixers are miniature broadband devices with maximum noise figures of 7.5 db and typical conversion losses of 6 - 7 db. Following conversion to the 30 MHz intermediate frequency, a FET driver was employed to couple the signal to the multi-section crystal band-pass filter depicted in figure 5. The nominal, 9 KHz (3db), system post-detection was established by this filter. The center frequency of the band-pass filter deviated no more than 450 Hz from the 30 MHz intermediate center frequency. The 9 KHz passband of the filter was sufficiently wide to handle Doppler frequency changes and the 3 KHz lobe-sweep offset frequency, but narrow enough to provide adequate signal-to-noise ratios in the recorded parameters.

A block diagram of the local oscillator subsystem employed in the 145.7644 MHz and 437.2932 MHz interferometer systems is shown in figures 10 and 14, respectively. To insure proper operating frequency of the receiver with minimum jitter and phase instability, the system required a high-Q frequency generating system utilizing oven-stabilized, crystal-controlled oscillators. The fixed crystal oscillator (XO) is stable to 2×10^{-8}/day, and $\pm 1 \times 10^{-7}$ over an ambient temperature range of 0°C to

50°C. The voltage-controlled, frequency-variable crystal oscillators (VCXO) have the same basic accuracy, and a voltage-controlled range of ±37.5 ppm for the 145.7644 MHz system and ±12.5 ppm for the 437.2932 MHz system. As shown in the diagram and associated referenced detailed schematic diagrams, the frequency output from the VCXO's and XO's is multiplied, filtered and distributed to the respective mixers at the 5 mw nominal drive level. Reactive power dividers and balanced mixers are used which have nominally 30 db isolation between ports, thereby maintaining sufficiently low cross-coupling to ensure independent phase measurements between adjacent antenna pairs.

The difference frequency between the XO and VCXO is amplified and fed into a synchronous detector. The synchronous detector provides an error output which drives the VCXO in a closed loop such that the difference frequency is stabilized to the 3.01 KHz reference clock frequency (see figures 10 and 25). The reference clock frequency of 3.01 KHz is derived from a 3.01 KHz crystal oscillator. An offset from 3.00 KHz was provided to avoid possible beat problems with the 30 MHz IF signal component. With allowance of sufficient time (10-15 minutes) for the crystal ovens to achieve their normal operating temperature, phase lock acquisition in normal operation was readily achieved.

Following conversion to the 30 MHz IF, the signal received from the respective antennas is amplified by standard IF amplifiers. These amplifiers have a nominal bandwidth of 2 MHz, a typical noise figure of 2.0 db, and a maximum power gain of 85 db. The dynamic range of AGC control is approximately 50 db.

2. Phase Measuring Subsystem

Two 3 KHz difference frequency signals (DET 1,2; DET 2,3) are formed by combining the IF signal component from the middle antenna leg with the IF signal component from each of the two end antenna legs as shown in figures 3, 6, and 7. The phase of this 3 KHz difference frequency relative to that of the 3 KHz clock is a measure of the signal path difference between respective interferometer elements. The isolating properties of the reactive power dividers, buffer amplifiers and mixers (cumulative), shown in figures 6 and 7, is such that negligible cross-talk exists between phase-measuring channels.

As shown in figure 14, the 3 KHz phase-measuring signal is then passed through a band-pass filter with a passband of 200 Hz, a zero-crossing detector, a one-shot, and finally a JK, flip-flop. This latter flip-flop is the heart of the phase meter. The JK flip-flop is cleared by the clock and preset by the positive going pulse output from the one-shot flip-flop. The average output from the flip-flop provides an analog measure of the phase difference between the 3 KHz signal and 3 KHz clock.

The purpose of the indicated low-pass filter is to limit the noise bandwidth, thereby maintaining noise errors within specifications. To realize a relatively flat pass-band over the range of expected data fluctuation, four-pole Butterworth low-pass filters were used, as shown in figures 3 and 4. A cutoff frequency was set at about 150 Hz and 60 Hz for the 145 MHz and 437 MHz system, respectively. These filters have a 24 db per octave rolloff above the cutoff point.

The system configuration is such that for a given change in wave-front incident angle (relative to the interferometer baseline) the measured phase differences $\phi_{1,2}$ and $\phi_{3,2}$ will be equal in magnitude and opposite in sign. The on-line measurement of the second difference in phase therefore entails the simple sum of $\phi_{1,2} + \phi_{3,2}$ as shown in the simplified block system diagram given in figures 1 and 13. Referring to figure 14, it is seen that the phase ambiguity channels denoted by $\phi_{i,j} + \pi$ are obtained by the use of additional flip-flops connected identically as the flip-flops associated with the parameter $\phi_{i,j}$ with the exception that the reference input clock signal is inverted.

3. Amplitude Measuring Subsystem

The amplitude portion of the lobe-sweep system is relatively straight-forward and is presented in the block diagrams given in figures 2 and 14, and the detailed schematics referenced in the block diagrams. Basically, for each beacon frequency, and associated with each antenna, there is an independent superheterodyne receiver. The received beacon signal is converted to 30 MHz, where the pre-detection bandwidth is narrowed to approximately 9 KHz with crystal filters. The signal is further amplified in a standard 30 MHz IF amplifier. The detected output of the 30 MHz amplifier is maintained at nearly constant level by employing the AGC

system shown in figures 1 and 14. The AGC operates off the incoherent background level. To avoid drifts in the AGC threshold caused by ambient temperature changes, a compensating diode was thermally coupled to the 30 MHz signal detector diode. As shown in figures 5 and 16, the compensating diode circuit is arranged such as to null the forward voltage variations due to temperature variations in the 30 MHz signal detector.

The post-detection bandwidth for amplitude measurement was established by low-pass, 4-pole Butterworth filters fed by the AGC line signal. These filters provided flat (to the cutoff points) passbands of 150 Hz and 60 Hz for the 145 MHz and 437 MHz systems, respectively.

The recorded element amplitude outputs were quasi-logarithmic, having approximately a 40 db dynamic range. In the computer reduction of the digitized amplitude data, the data were corrected to true db, utilizing a look-up table comprised of amplitude calibration points listed at 10 db increments. Linear interpolation was used to arrive at the true db level of the signal.

E. MAJOR COMPONENTS PARTS LIST

The major components used in the interferometer system are listed in Table III. As shown, the list includes the description of the component, the manufacturer's identification, and the figure in which the part is referenced.

III. FIELD OPERATION OF LOBE-SWEEP INTERFEROMETER EQUIPMENT

A. GENERAL

The purpose of this section is to outline the various tests and procedures employed in the calibration and checkout of the interferometer system. The interferometer receiver was operated in the field during the SECEDE II test series as part of the beacon transmission experiment. The interferometer receiver was located with a dispersive phase receiver at a site favorable for observing occultation effects (center station No. 2, Wewahitchka N). In the SECEDE II test observations, the interferometer was operated at 145.7644 MHz and 437.2932 MHz, and consisted of three equally-spaced receiving elements set in a line one hundred meters apart.

COMPONENT DESCRIPTION	MANUFACTURER'S IDENTIFICATION	QUANTITY	FIGURE NO. REFERENCED
Oven-stabilized crystal oscillator 101.8233 MHz, 3×10^{-8}/day	Vectron Mod. No. CO-223	1	6
Oven-stabilized, voltage-controlled crystal oscillator, 101.8233 MHz, 3×10^{-8}/day, range of control ±12.5 ppm	Vectron Mod. No. CO-221	1	6
Oven-stabilized crystal oscillator 57.8822 MHz, 3×10^{-8}/day	Vectron Mod. No. CO-223	1	5
Oven-stabilized, voltage-controlled crystal oscillator, 57.8822 MHz 3×10^{-8}/day, range of control ±37.5 ppm	Vectron Mod. No. CO-221	1	5
Antenna pre-amplifier, cf 437.3 MHz 3 db bandwidth 10 MHz	C-Cor Mod. No. 2202A	3	3
Antenna pre-amplifier, cf 145.8 MHz 3 db bandwidth 13 MHz	C-Cor Mod. No. 2579	3	3
30 MHz IF amplifier, gain 80 db, 3 db bandwidth 2 MHz	RHG Mod. No. EVT3002	6	1, 5, 6
Test oscillator amplifier cf 300 MHz, BW 200 MHz	Fairchild Mod. No. MHZ-300B-02	1	25
30 MHz cf, BW 9 KHz crystal IF filters	Bulova Mod. No. 954	6	1, 4
437.3 MHz double balanced mixer	Anzac Mod. No. MAC50	3	4
Double balanced mixer	Anzac Mod. No. MAC51	5	4, 5, 9, 11
Log-periodic dipole antenna assembly	Advant Mod. No. 5-057001A	3	1, 2, 3, 25
Power divider 20-200 MHz	Merrimac Mod. No. PD-20-110	5	5, 6, 9
Power divider 200-400 MHz	Merrimac Mod. No. PD-20-300	3	11
Bandpass filter cf 407.3 MHz 3 db BW 418-396 MHz	Texscan Mod. No. 3BC407.3	2	11
Bandpass filter cf 115.8 MHz 3 db BW 113-119 MHz	Texscan Mod. No. 3BC115.8	2	9
Bandpass filter cf 437.3 MHz 3 db BW ±10% cf	Texscan Mod. No. 4BE437.3	1	25
Bandpass filter cf 145.8 MHz 3 db BW ±10% cf	Texscan Mod. No. 4BE145.8	1	25

TABLE III - MAJOR COMPONENTS PARTS LIST

The center element was at the approximate location of the dispersive phase receiver. The interferometer antennas were mounted on remotely controlled elevation-azimuth rotators approximately forty feet above the ground. Measurements consisted of element amplitudes and phase differences between adjacent element pairs. At the time of occultation, full-scale variation in phase corresponded to approximately 23 milliradians at 145 MHz and 7.5 milliradians at 437 MHz.

B. SIGNAL CALIBRATION TEST SOURCE

The calibration test source was used to provide a known signal level at the 145.7644 MHz and 437.2932 MHz beacon frequencies. The method of utilization and general operation configuration of the test oscillator system is given in the block diagram shown in figure 26. The circuit schematic of the crystal oscillator test source, and associated frequency multipliers, is given in figure 27. Fine tuning of the oscillator was accomplished by pulling the crystal frequency with the variable inductor shown in the drain circuit of *Q1*.

1. Test Antenna Mode

As indicated in figure 25, the test oscillator system operates in two basic modes. With *S3* closed, the test oscillator signal drove one of the two ground-plane (145 MHz, 437 MHz) antenna assemblies which were mounted forty feet above ground on a pole located at the apex of an equilateral triangle. The base of the triangle was formed by the two-hundred-meter interferometer baseline.

Operating in the "test antenna mode", the interferometer receiver antennas were pointed at the test antenna, and the approximate signal levels were checked at the quasi-logarithmic element amplitude outputs at the three interferometer antenna locations. This test provided a qualitative measure of the system performance for a signal received by the interferometer antennas. Malfunctions in antenna connectors, hybrid junctions in the antennas, etc. were isolated by these tests. Precise system gain calibration checks could not be made in the test antenna mode due to problems associated with ground reflections and reflections from nearby surface objects.

2. Test System Mode

Referring again to figure 25, with *S3* open and *S1*, *S2* closed, the calibration oscillator operates in the "test system mode". In this mode an accurately known signal level is coupled directly into the receiver pre-amplifier inputs via the pre-amplifier housing antenna units shown in figures 4 and 26. With proper account taken of coaxial line loss, attenuation from power dividers and isolators, and antenna gain, step attenuator readings (see figure 25 for location of step attenuators) equivalent to a test beacon at three hundred km range were established. The majority of the pre-shot systems tests were carried out using the "test system mode". Necessary system calibration adjustments were thereby established, as was the determination that the system operated to specifications.

Prior to the above tests, the test oscillator output was monitored and the frequency adjusted to within 1000 Hz of the nominal frequency of the beacon signal. The output level was calibrated, using a spectrum analyzer, and comparing the test oscillator output with an external test oscillator of known output level.

C. AMPLITUDE CALIBRATION PROCEDURE (reference figure 15, 145 MHz system; figure 16, 437 MHz system)

With the system in the "test system mode", the dynamic range of amplitude measurement was adjusted to respond to a 40 db range of input signal. The threshold detection level was adjusted with *R1* as shown in figures 15 and 16 to approximately 20 db below the level of beacon signal expected at the three hundred km range. The AGC loop gain, although adjustable by *R2*, was left at the factory setting. The output offset and output gain are controlled by *R3* and *R4*, respectively. The gain and offset were set so that the output to the recording system (pin 20) varied from -1.4 to +1.4 volts, corresponding to a change in input signal level ranging from threshold to threshold +40 db. The amplitude response was thus quasi-logarithmic over a dynamic range of 40 db. Amplitude calibration points of voltage output for 10 db input steps over the 40 db dynamic range were obtained prior to and following each field test event.

D. PHASE METER CALIBRATION PROCEDURE

A block diagram of the test configuration for phase meter calibration is shown in figure 28. An external variable audio oscillator is synchronized to the 3 KHz reference clock. With the oscillator set at approximately the 3 KHz reference frequency, the signal is fed via a variable phase-shifter (see figure 28 for the test circuit) to pin 3 of the phase meter under test (see figure 27 and figures 18 through 21). The phase of the 3 KHz signal relative to the reference clock is adjustable over a 2π range by varying both the audio oscillator within the lock-in range, and the variable phase shift control in the test circuit of figure 29. The above procedure simulated a phase variation caused by beacon motion over at least one interferometer fringe, and thus provided a technique for adjusting the calibration setting of the phase meter.

The calibration was adjusted so that over a 2π phase variation, the output of the phase meter changed by ± 1.4 volts. This was accomplished by varying the offset ($R1$) and gain ($R2$) of the respective phase meter following the low-pass filter (see applicable figures 16, 17, 22, 23) so that proper full-scale operating range was achieved. Proper phase calibration was verified by observing the phase variation obtained from the beacon signal as the beacon passed through the interferometer fringe pattern. Peak-to-peak phase output variations of ± 1.4 volts corresponding to beacon motion, confirmed proper system operation.

E. DYNAMIC RESPONSE TEST - PHASE AND AMPLITUDE

For these tests the system was operated in the "test system mode" with the amplitude level set to correspond to the beacon signal level at the three hundred km range. The test system of figure 30 was used to insert into the system a cyclically varying attenuation or phase shift. The external jumper was removed in the mixer-filter unit shown in figure 5, and the voltage variable attenuator or phase shifter inserted at this point (see also figure 30). Both element amplitude output channels and phase output channels were monitored with a direct coupled oscilloscope. The audio oscillator was changed in frequency from approximately 4 Hz to the observed cutoff point where the response was 3 db down.

The introduction of small amplitude and phase variations was necessary to these measurements. Small amplitude variations ensured measured output variations linear with input level change; small phase variations minimized problems of residual amplitude changes generated within the indicated phase shifter for introduced phase variations greater than about 10 degrees. The magnitude of the phase or amplitude variation introduced was determined by the output level of the audio generator shown in figure 30.

F. XO AND VCXO OPERATION

The temperature of both the crystal oscillator (XO) and the voltage variable crystal oscillator (VCXO) is stabilized with a proportional control oven system, and normally there is no need for internal adjustment of the fine frequency. There is, however, provision for fine frequency adjustment on the respective VCXO or XO unit if such is necessary.

Following warm-up stabilization of the crystal ovens, the VCXO should be locked to a 3 KHz difference frequency between the local oscillator signals derived from the XO and VCXO signal sources. Adjustments to the closed-loop parameters of the phase lock system can be made to achieve lock and stable lock-in performance. This is accomplished by varying loop gain (*R1*) and frequency offset (*R2*) until proper performance is achieved. Lock-in is verified by comparing the output *DF-1A* or *DF-1B* shown in figures 9 or 11, respectively, with the appropriate 3 KHz reference clock and testing for SYNC condition.

G. OPERATION TEST AND MEASUREMENT SCHEDULE

The test and/or calibration procedures carried out in the field at 24 hours and 4 hours prior to a scheduled beacon test shot are summarized in Table IV. Those operations requiring the test oscillator are noted, together with the time required to accomplish a specified function. The calibration and test procedures required in the maintenance and operation of the data recording equipment is not discussed here. This information is discussed in the manufacturer's instruction manuals covering the equipment of interest.

TEST OR CALIBRATION	TEST OSCILLATOR ON	TIME REQUIRED (Minutes)	T_o - 24H	T_o - 4H
Precision Instruments recorder calibration		120	x	
Quick test Precision Instruments recorder calibration		15		x
Ampex recorder calibration		60	x	
Quick test Ampex recorder calibration		15		x
Techni-rite recorder calibration		15	x	x
XO and VCXO frequencies test and check for lock-in		5	x	x
Phase calibrate phase meter		15	x	x
Amplitude calibration	x	5	x	x
Test signal through interferometer antennas	x	20	x	x
Measure phase variation over 40 db range of amplitude	x	5	x	x

TABLE IV - OPERATION SCHEDULE FOR PRE-SHOT TESTS AND CALIBRATIONS

IV. CONCLUSION

The lobe-sweep interferometer equipment described herein operated in accordance with specifications during field operations associated with the SECEDE II test series. Test measurements in the field prior to data acquisition indicated that a problem existed in the antenna connectors caused from the accumulation of water. This problem was subsequently eliminated by coating the connectors with a sealing compound.

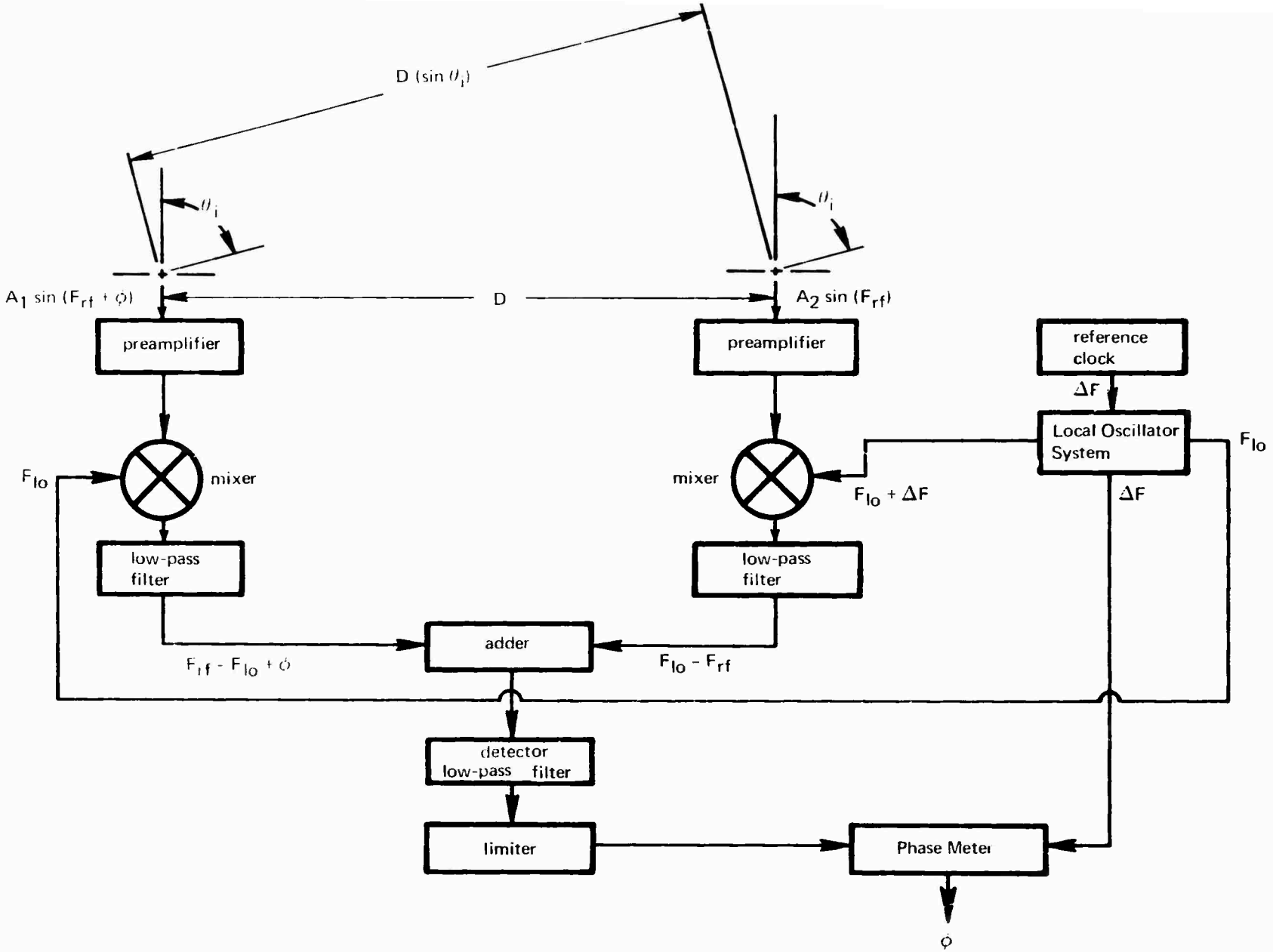

Figure 1: Operating Principle—Lobe-Sweep Interferometer

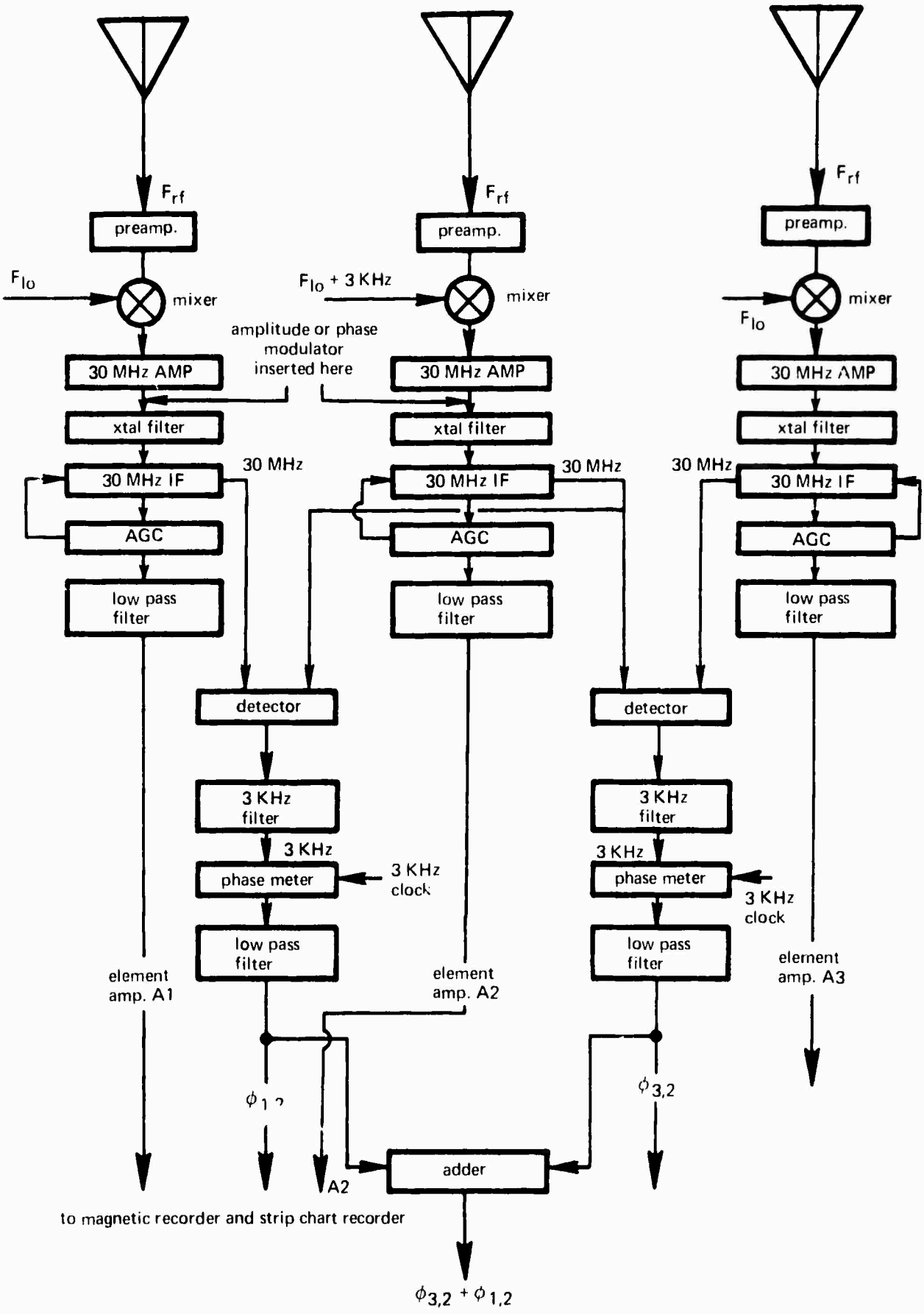

Figure 2: Simplified Block Diagram of Interferometer System

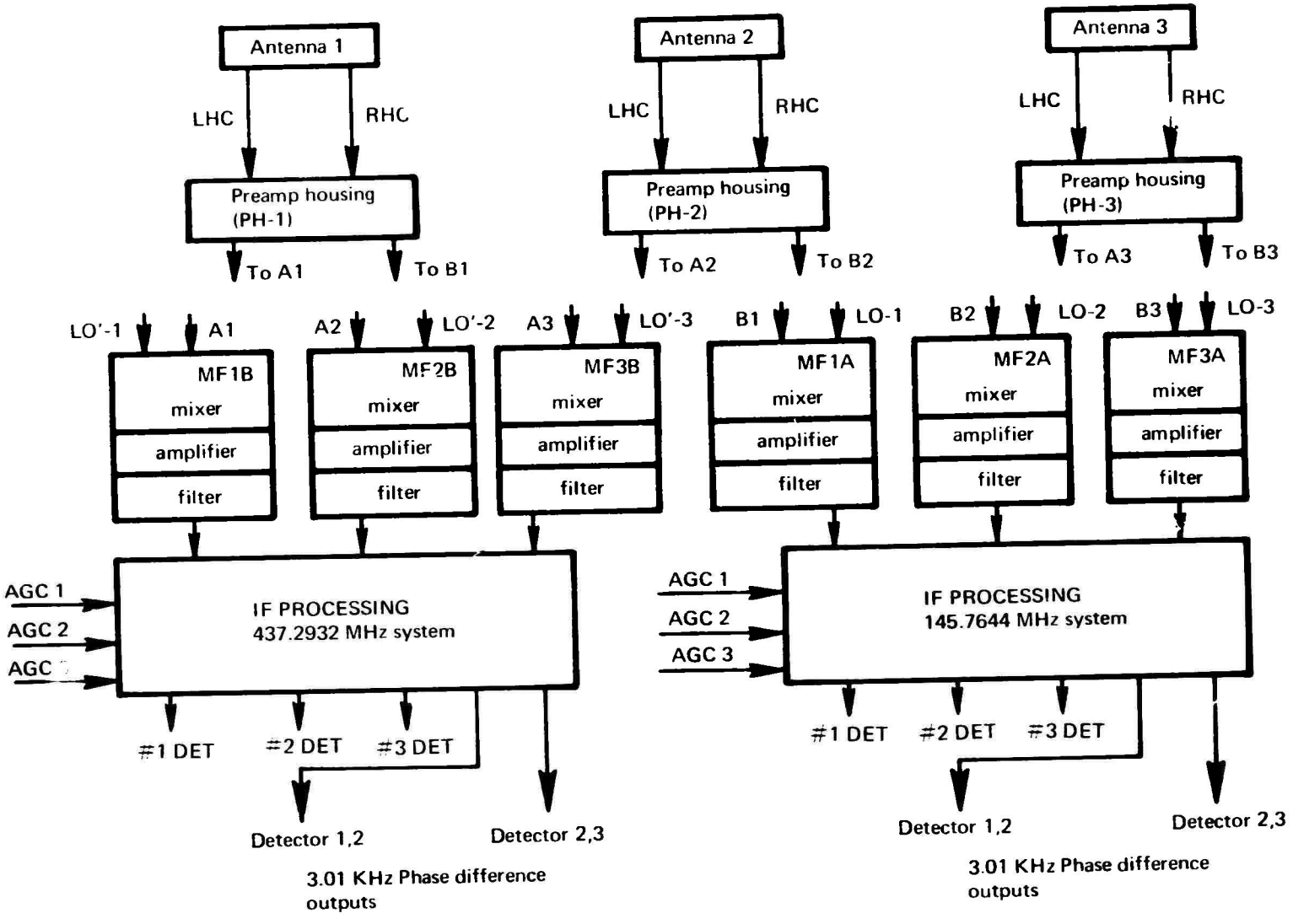

RHC = right hand polarization
LHC = left hand polarization
LO-1, LO-3 = 115.7644 MHz local oscillator signal

LO-2 = 115.7674 MHz local oscillator signal
LO'-1, LO'-3 = 407.2932 MHz local oscillator signal
LO'-2 = 407.2962 MHz

Figure 3: Block Diagram of the RF Subsystem

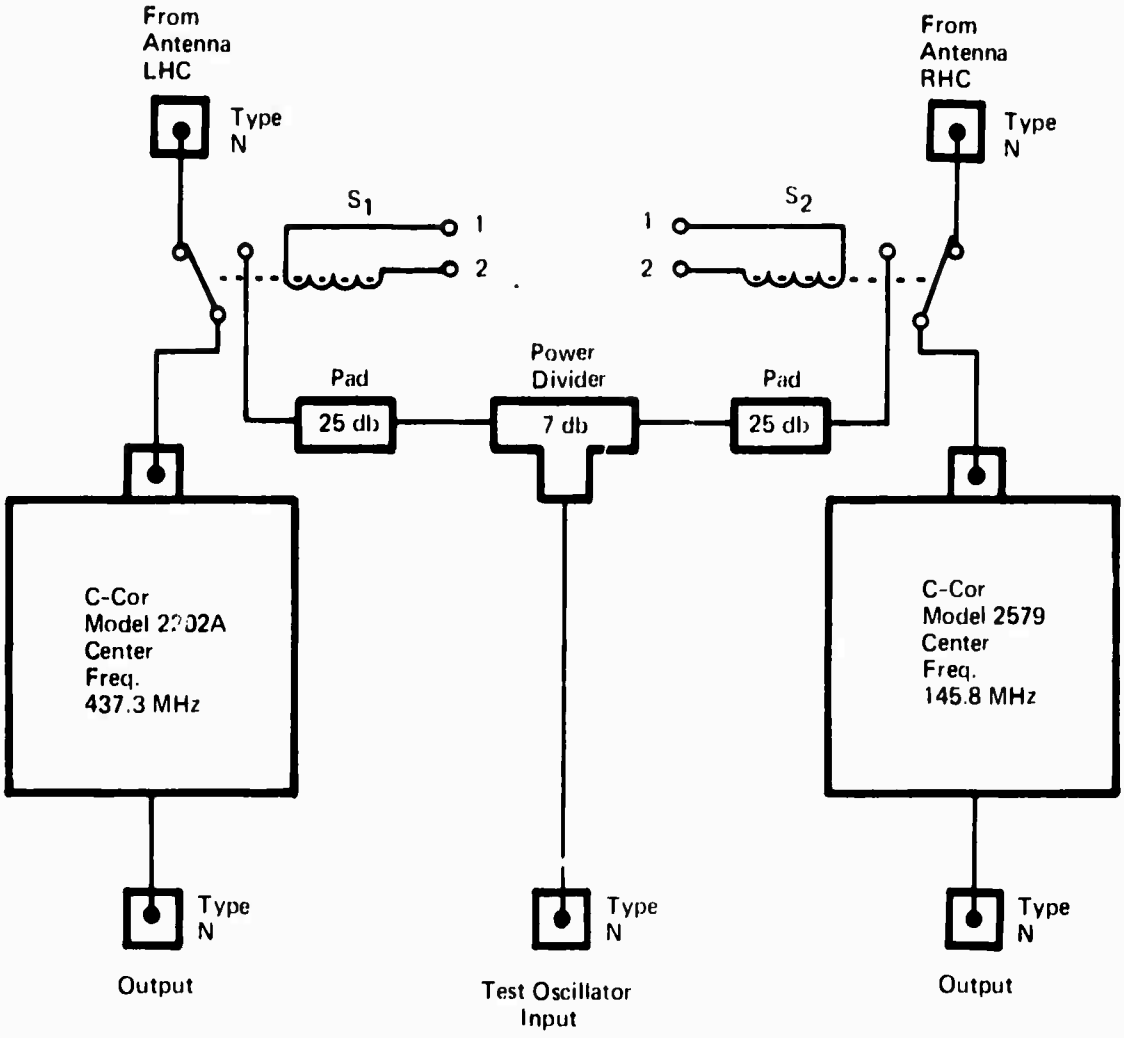

S_1, S_2 - Coaxial Switch
28 vdc Actuation Voltage

RHC = Right Hand Polarization
LHC = Left Hand Polarization

Figure 4: Preamplifier Housing PH Series

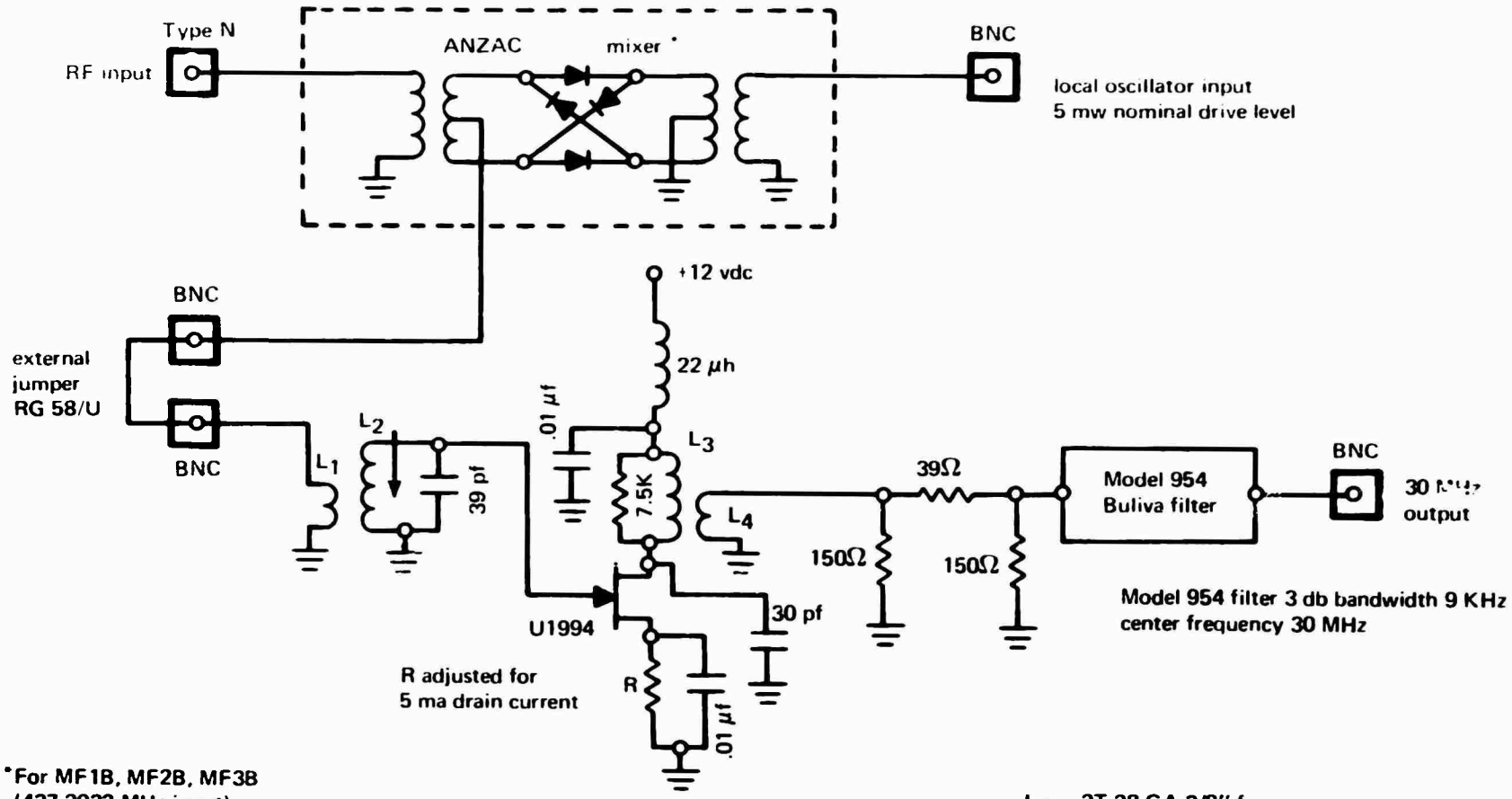

*For MF1B, MF2B, MF3B
(437.2932 MHz input)
Anzac mixer MAC 50

For MF1A, MF2A, MF3
(145.7644 MHz input)
Anzac mixer MAC 51

L_1 2T 28 GA 3/8" form
L_2 10T 28 GA Bifiliar wound with L_1
L_3 10T 28 GA 3/8" form
L_4 2T 28 GA Bifiliar wound with L_3

Figure 5: Mixer-Filter Unit MF Series

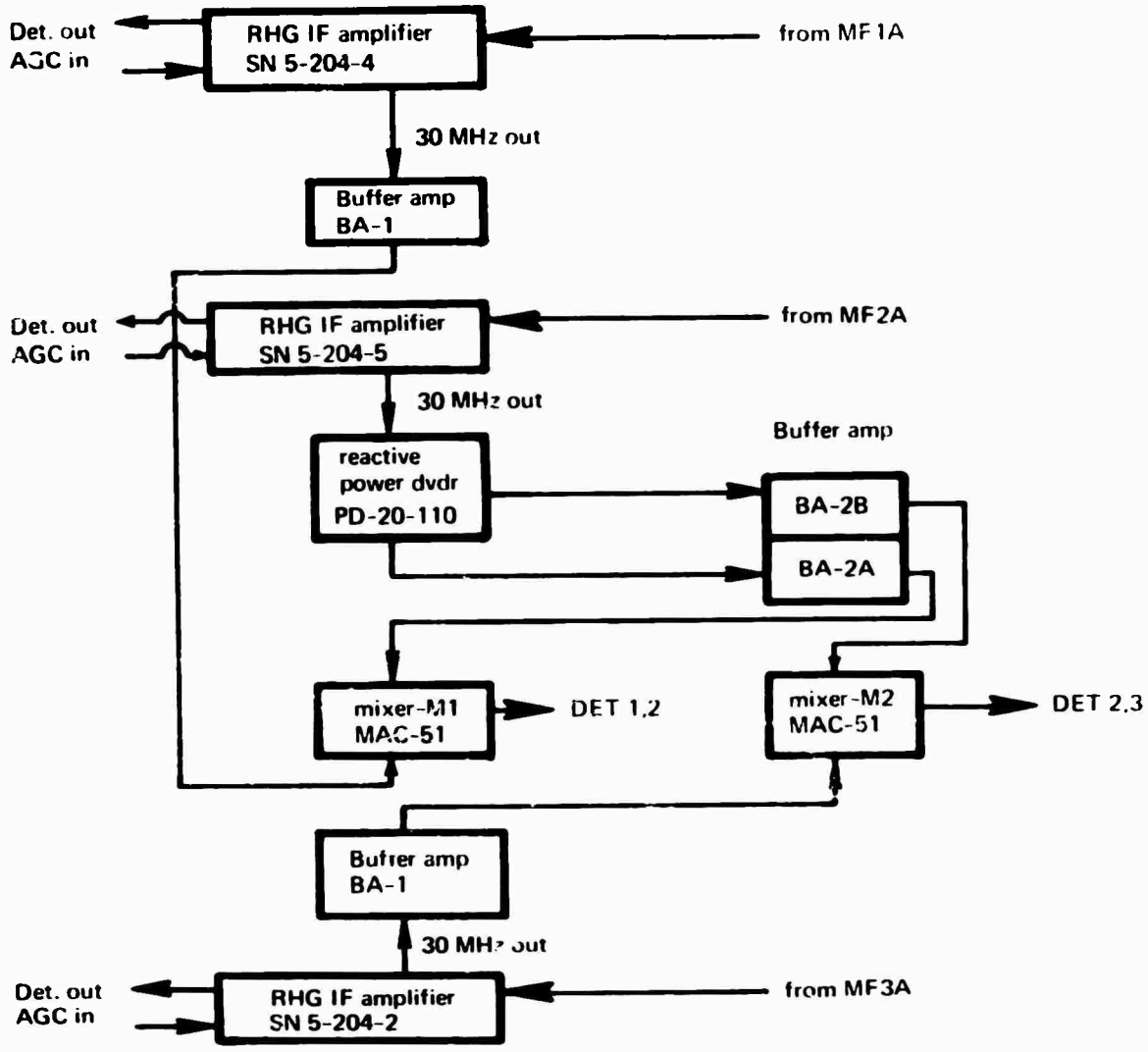

Figure 6: Block Diagram—IF Processing for the 145.7644 MHz System

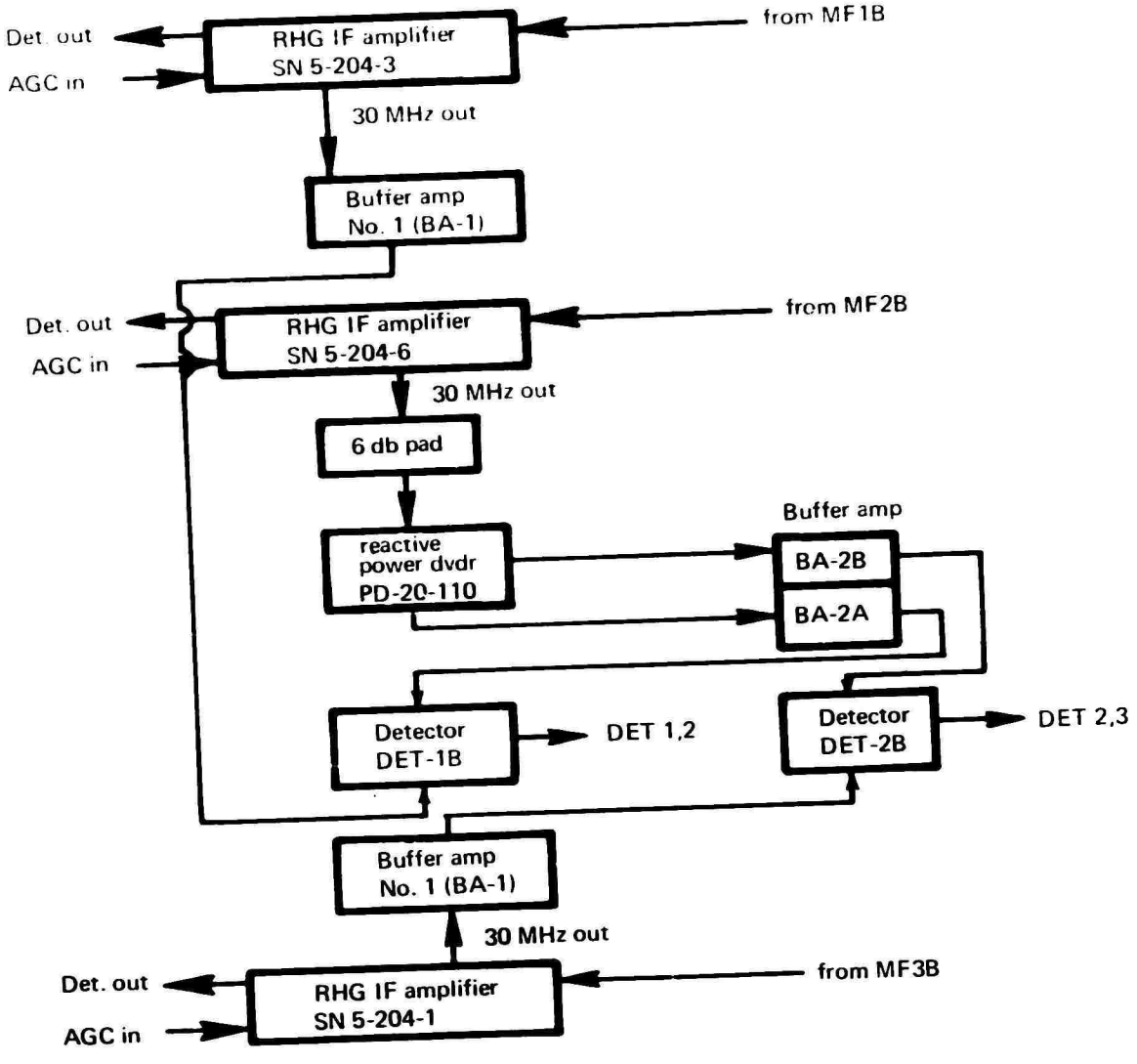

Figure 7: Block Diagram—IF Processing for the 437.2932 MHz System

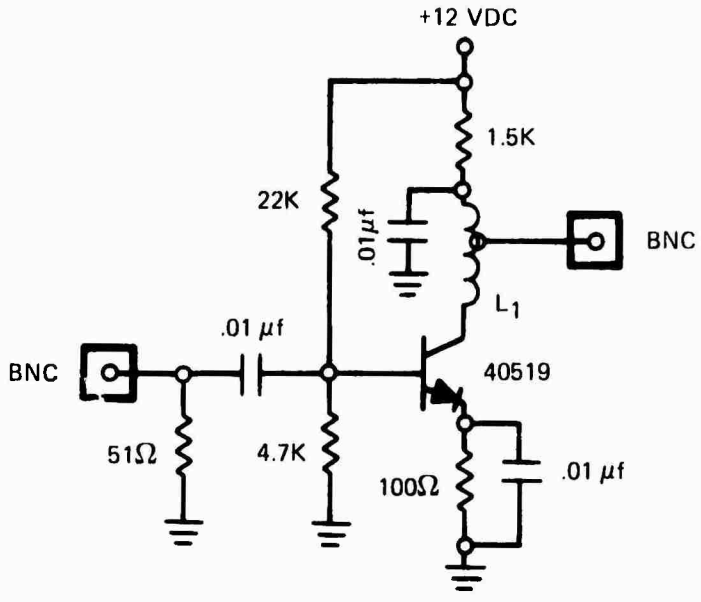

L_1 23T 32 GA TAP 3T FROM GROUND

BUFFER AMPLIFIER BA-1

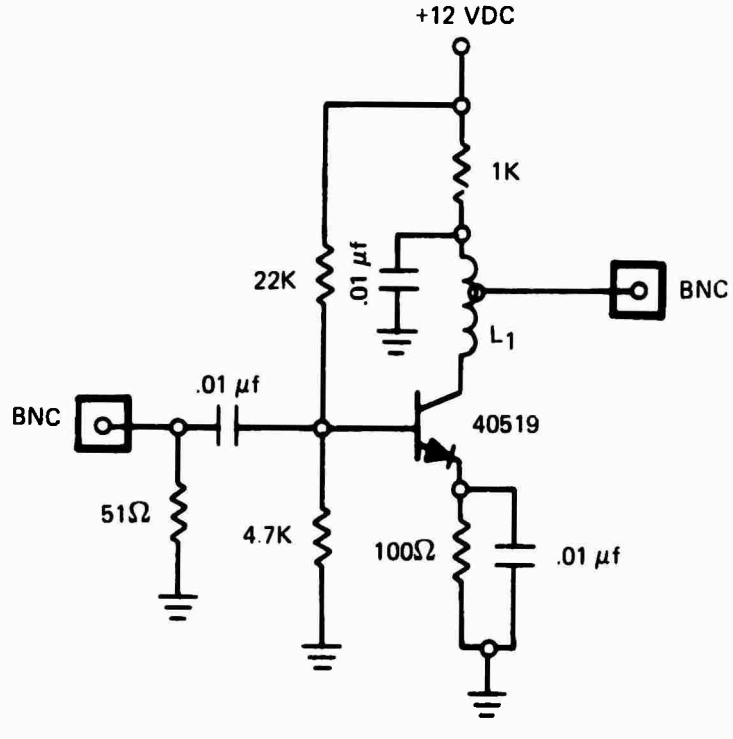

L_1 18T 32 GA TAP 2T FROM GROUND

BUFFER AMPLIFIER BA-2A, BA-2B

Figure 8: Buffer Amplifiers, BA-1, BA-2A, BA-2B

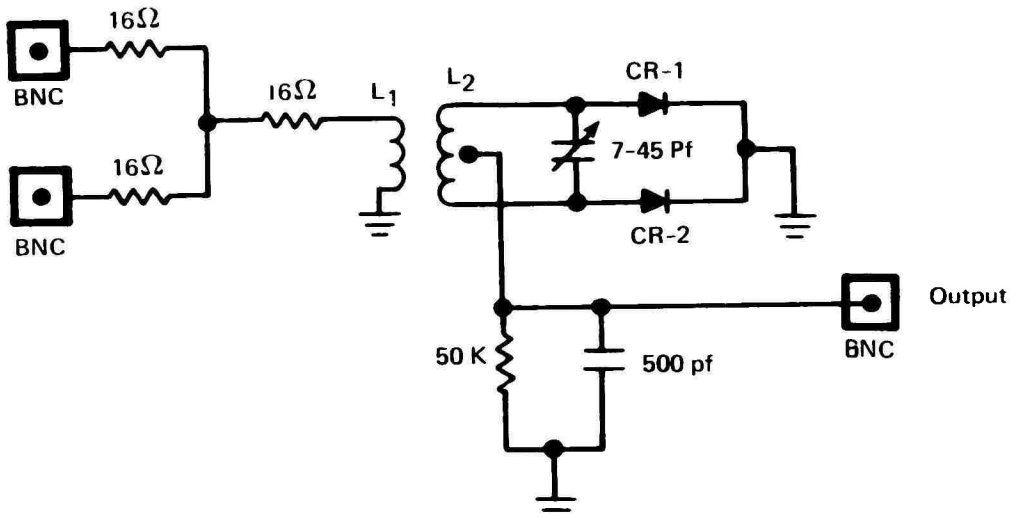

L_1 2T 28 GA 3/8" Dia.
L_2 lot 28 GA Bifiliar Wound with L_1
CR-1, CR-2 HP 5082 Hot Carrier

Figure 9: Detector 1B, 2B

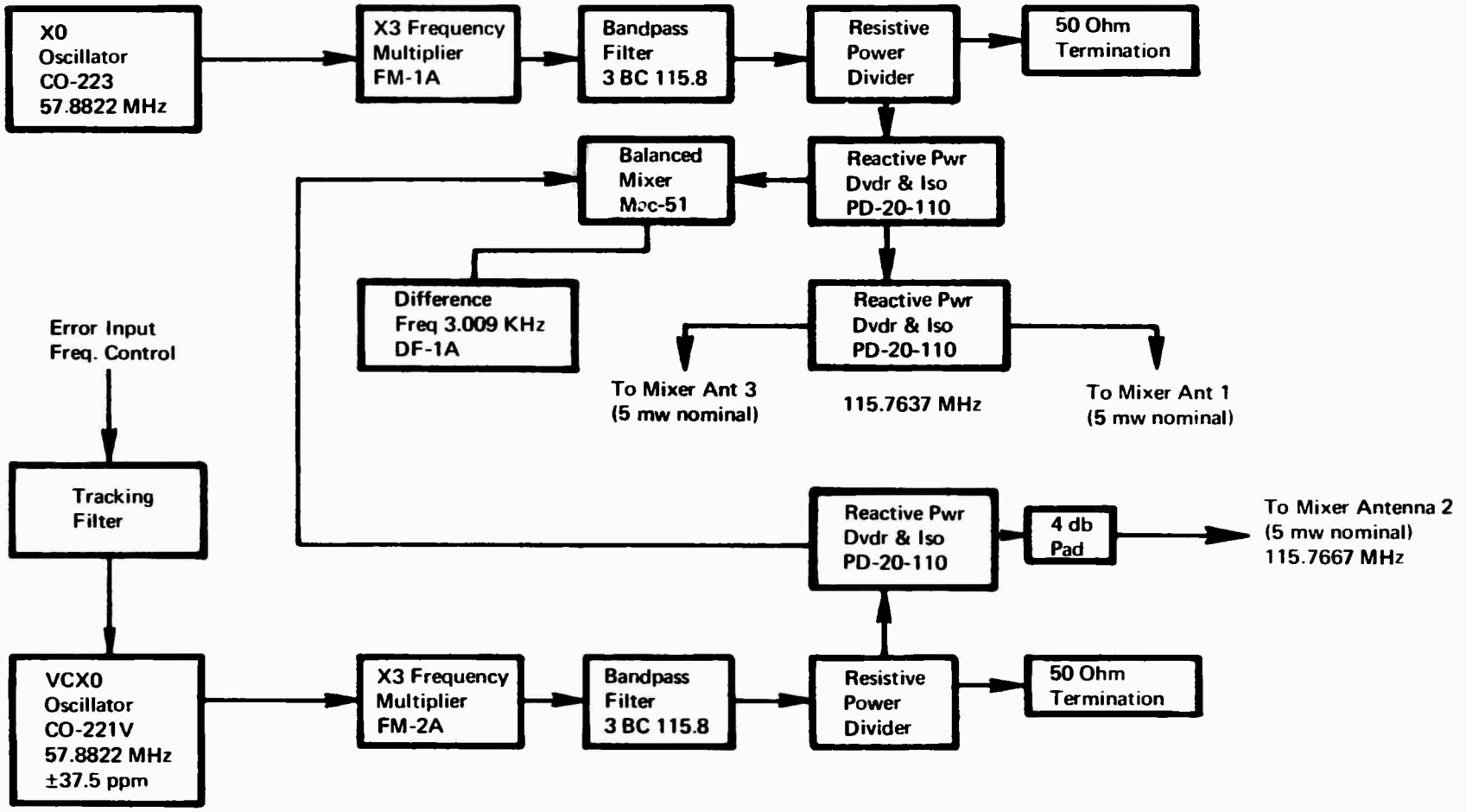

Figure 10: Block Diagram of 145.7644 MHz Local Oscillator Subsystem

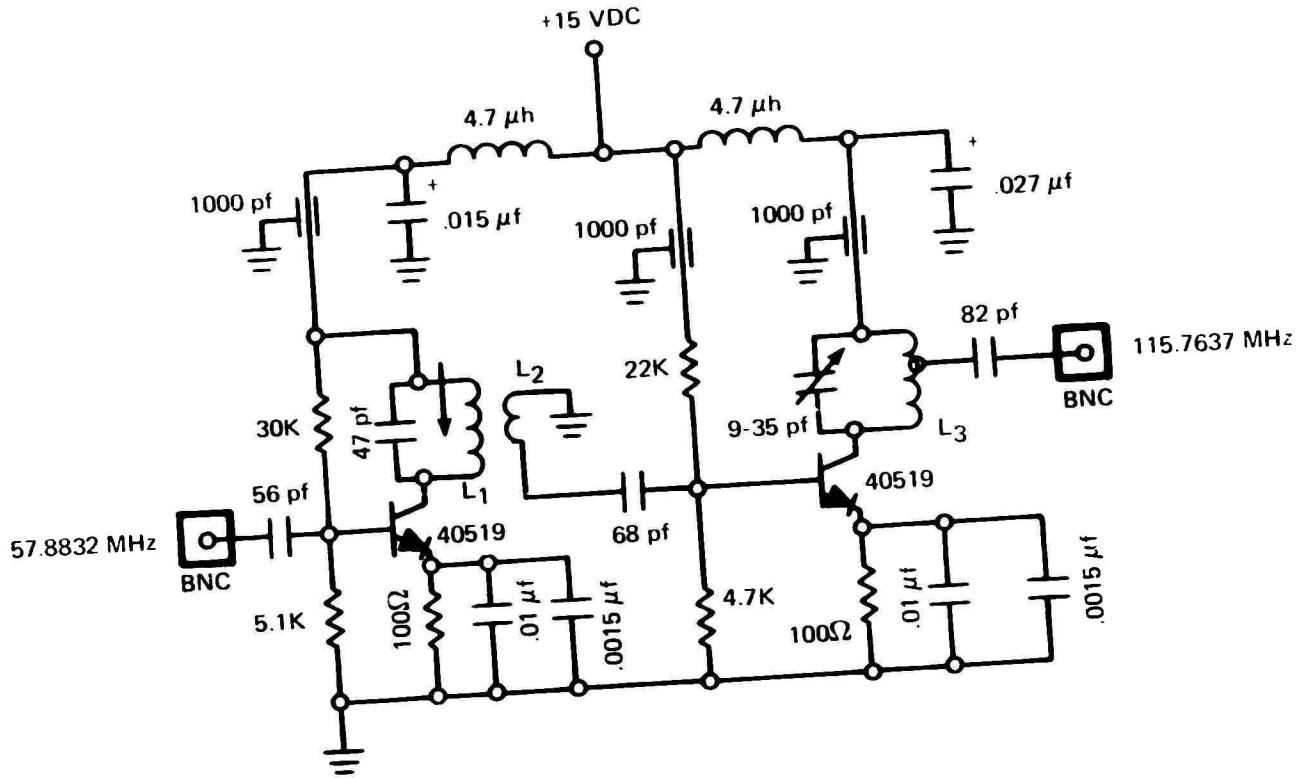

L_1 5T 26 GA on Miller 1/4" form
L_2 2T 24 GA Bifilar wound on low end of L_1
L_3 4T 16 GA 1/2" air core tapped 3T from low end

Figure 11: Frequency Multiplier, FM1A, FM2A

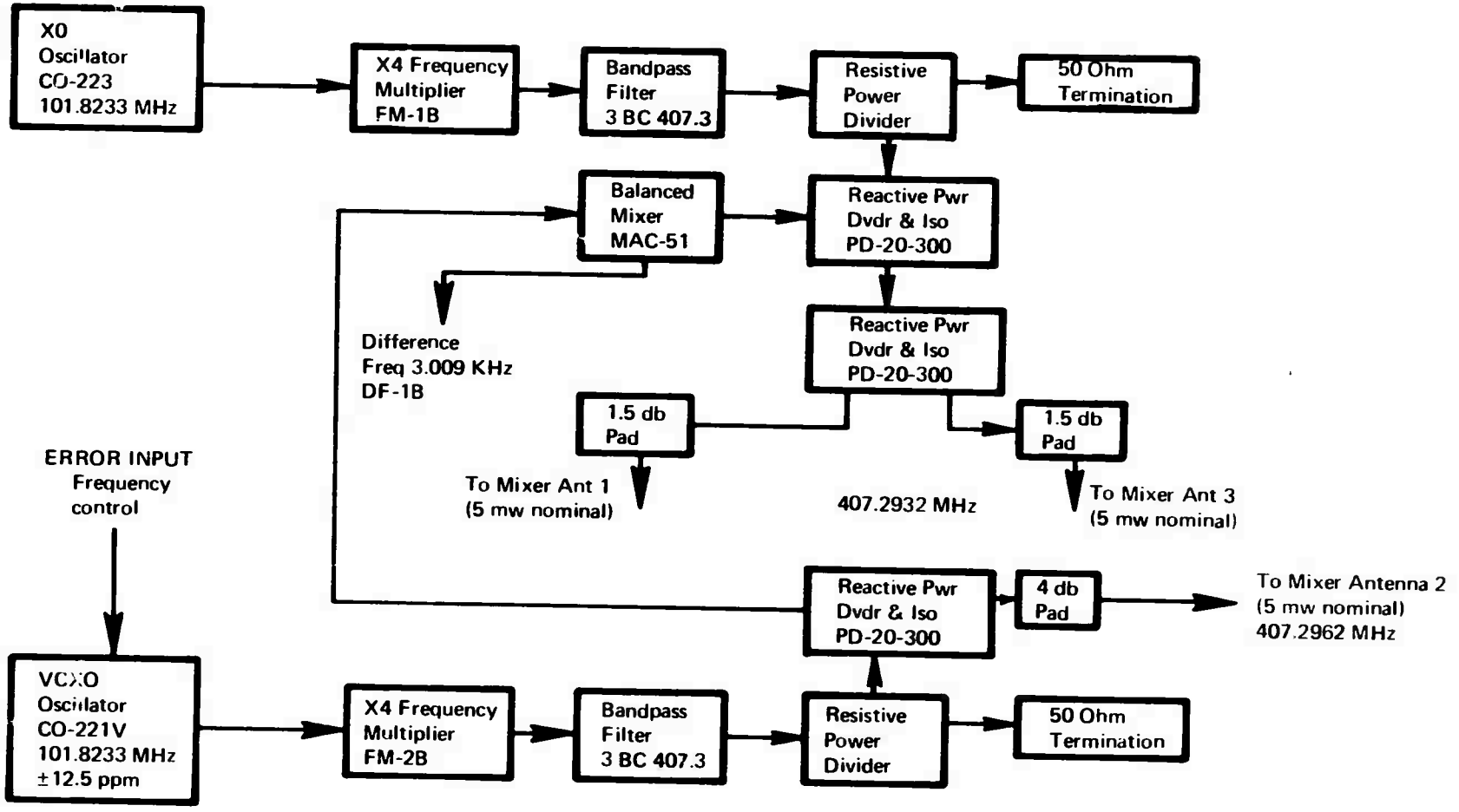

Figure 12: Block Diagram of 437.2932 MHz Local Oscillator Subsystem

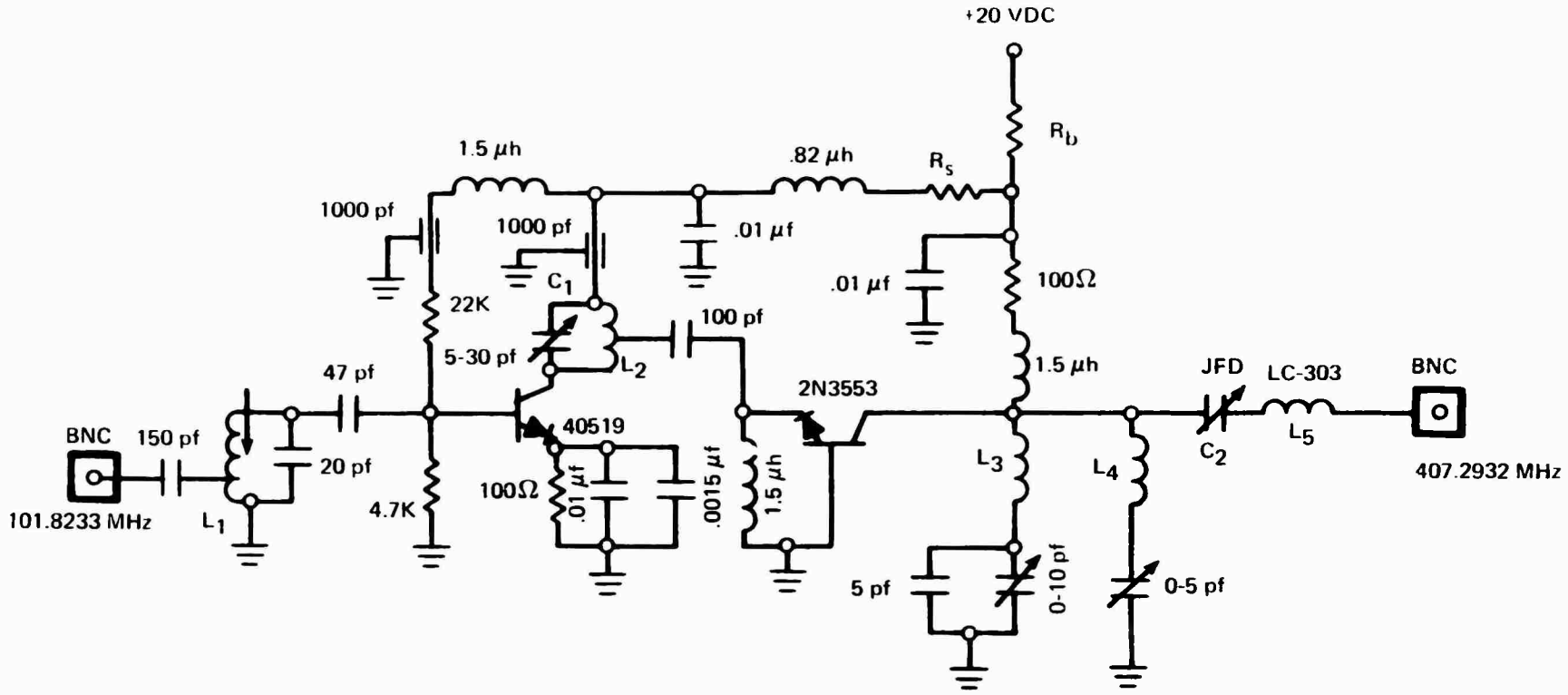

L_1 5T 16 GA on 1/4" ceramic form tap 2 3/4 turns from ground

L_2 T5 16 GA on 1/4" ceramic form tap 1 turn from R.F. ground

L_3 6T 16 GA on 5/16" air form

L_4 4T 16 GA on 5/16" air form

C_1 Miniature ceramic trimmer

C_2 L_5 Series resonant at 407 MHz JFD LC-303

	FM1B	FM2B
R_s =	1500Ω	810Ω
R_b =	75Ω	0

Figure 13: Frequency Multiplier, FM1B, FM2B

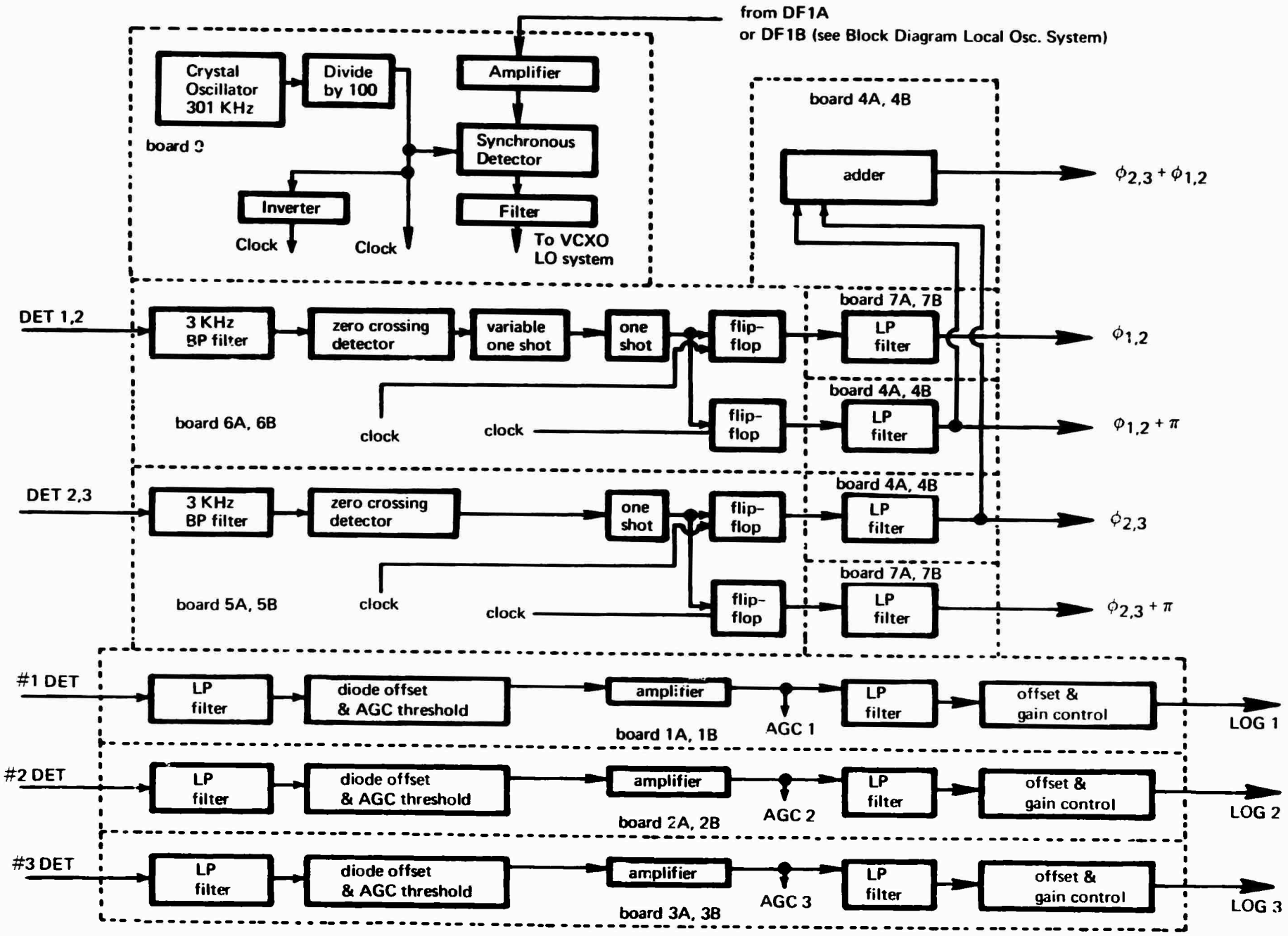

Figure 14: Block Diagram of Audio Subsystem

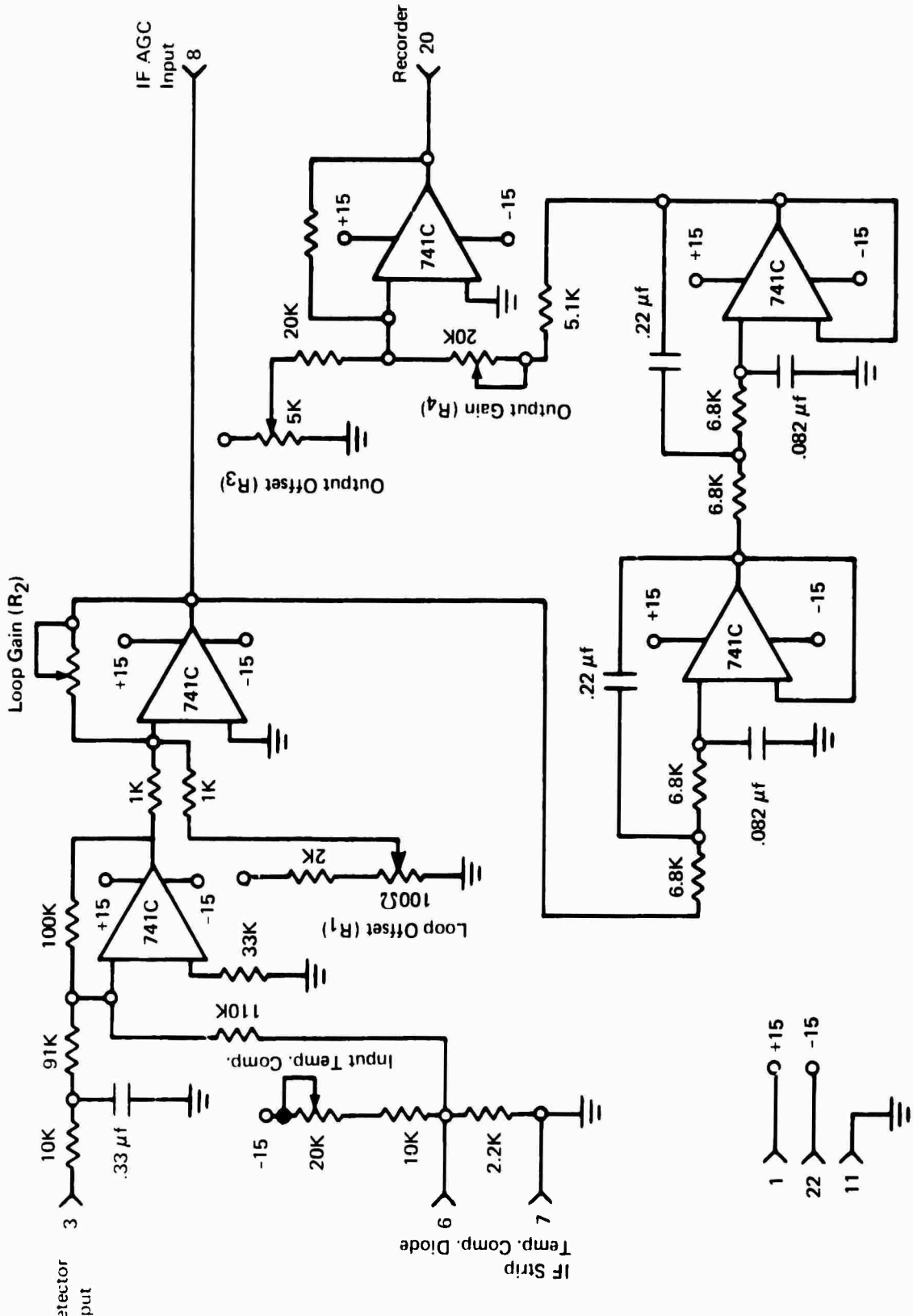

Figure 15: Board 1A, 2A, 3A–145.7644 MHz Audio Subsystem

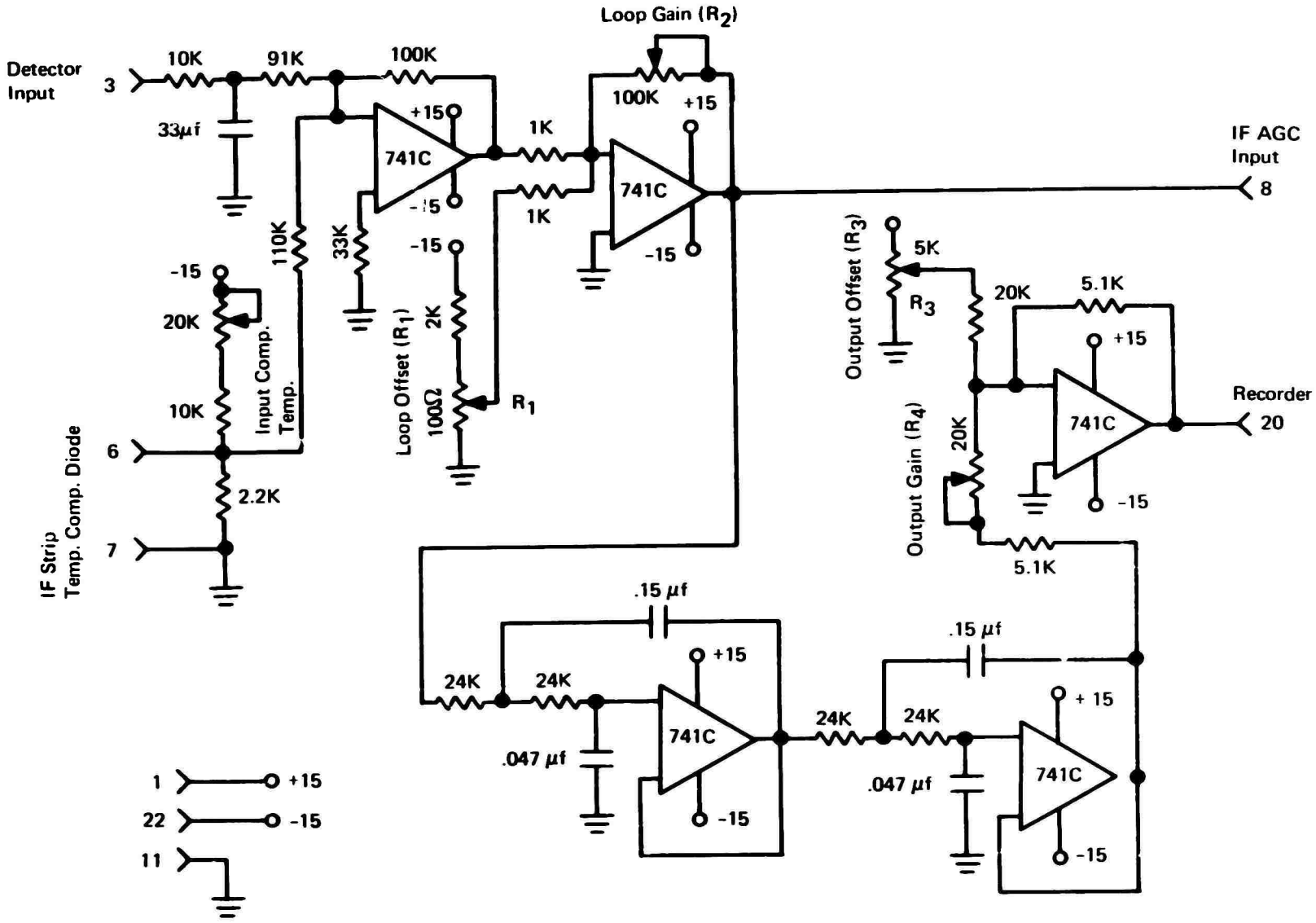

Figure 16: Board 1B, 2B, 3B–437.2932 MHz Audio Subsystem

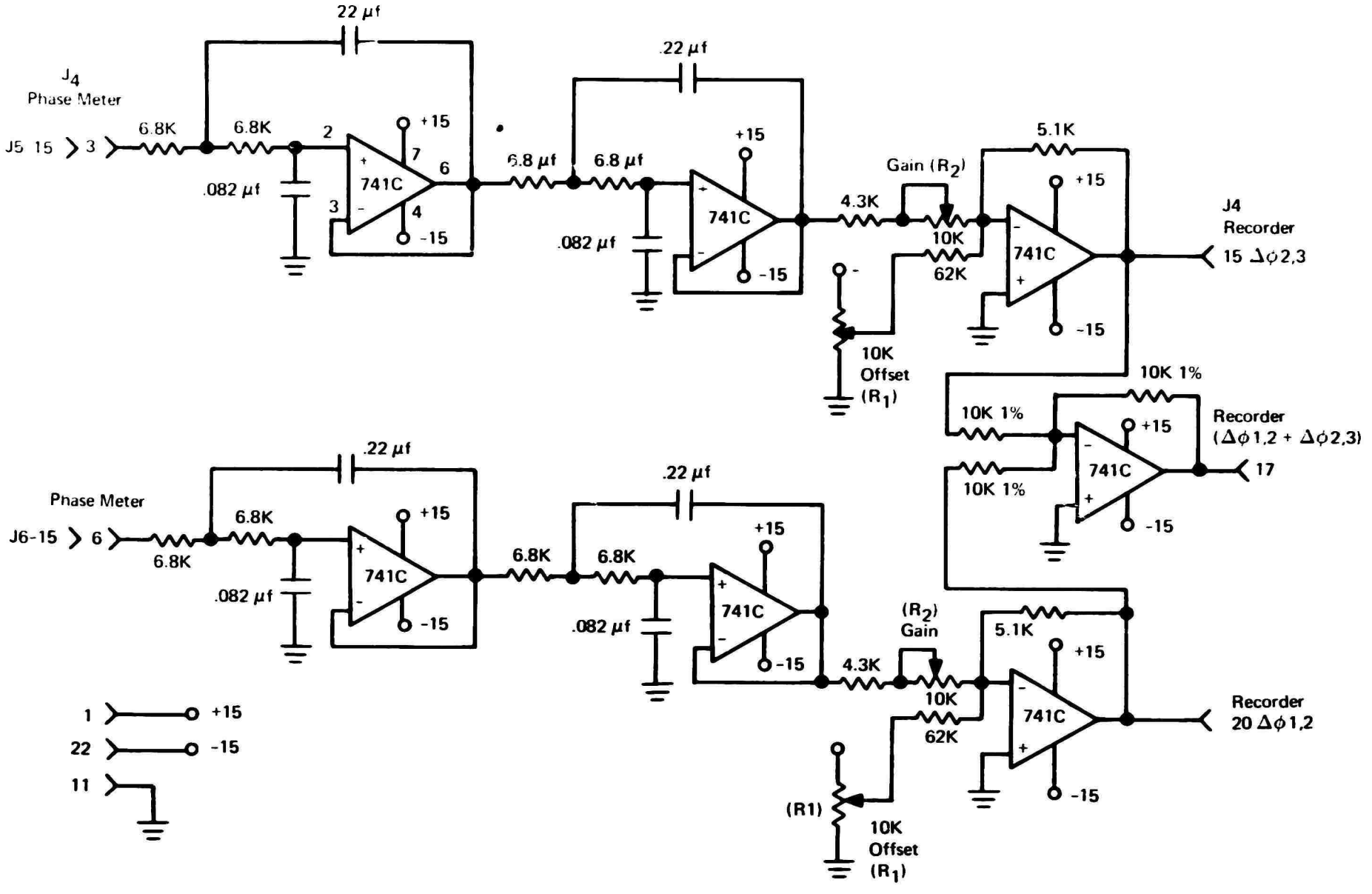

Figure 17: Board 4A—Low-Pass Filter and Adder—145.7644 MHz Audio Subsystem

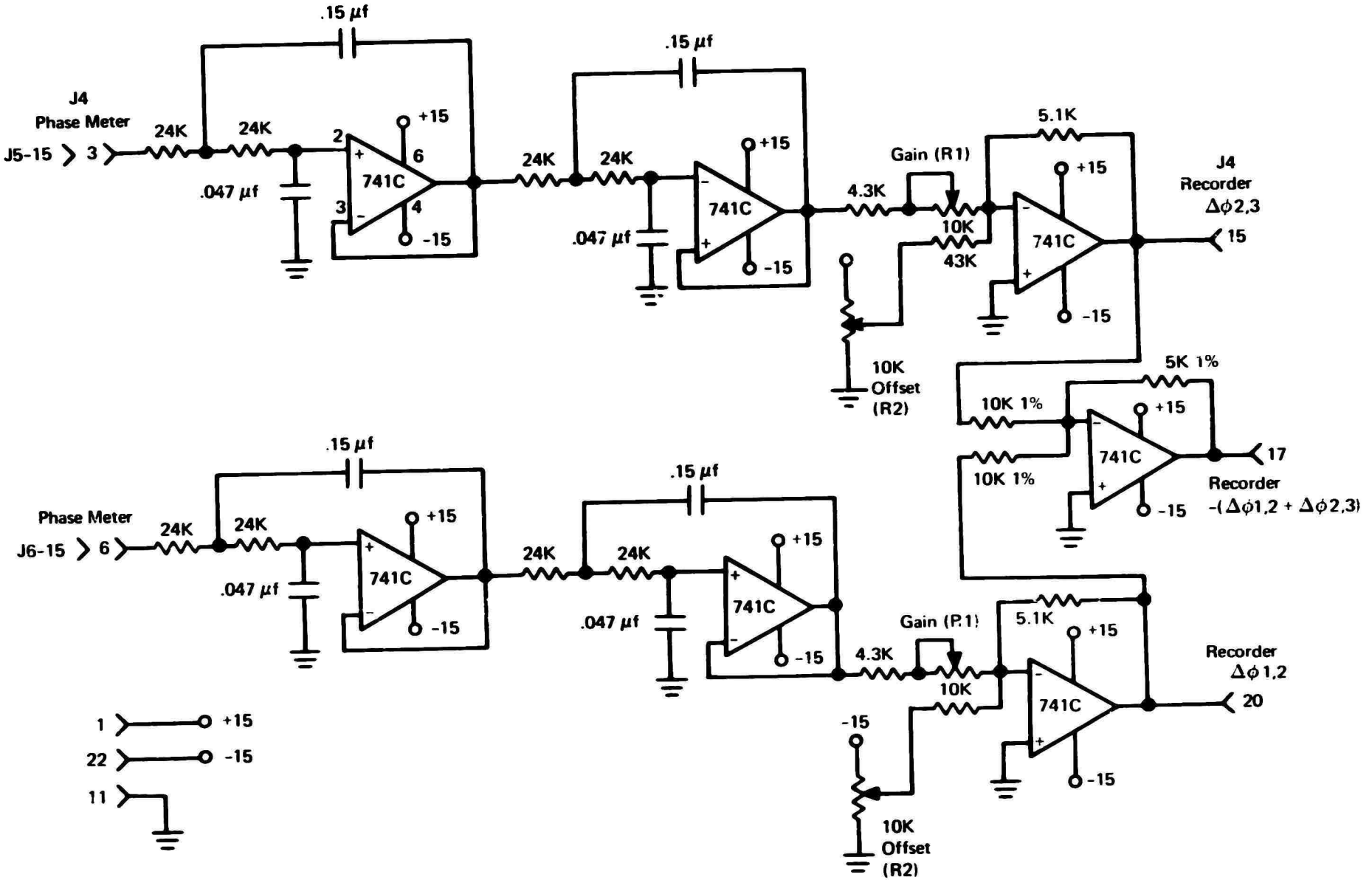

Figure 18: Board 4B—Low Pass Filter and Adder—437.2932 MHz Audio Subsystem

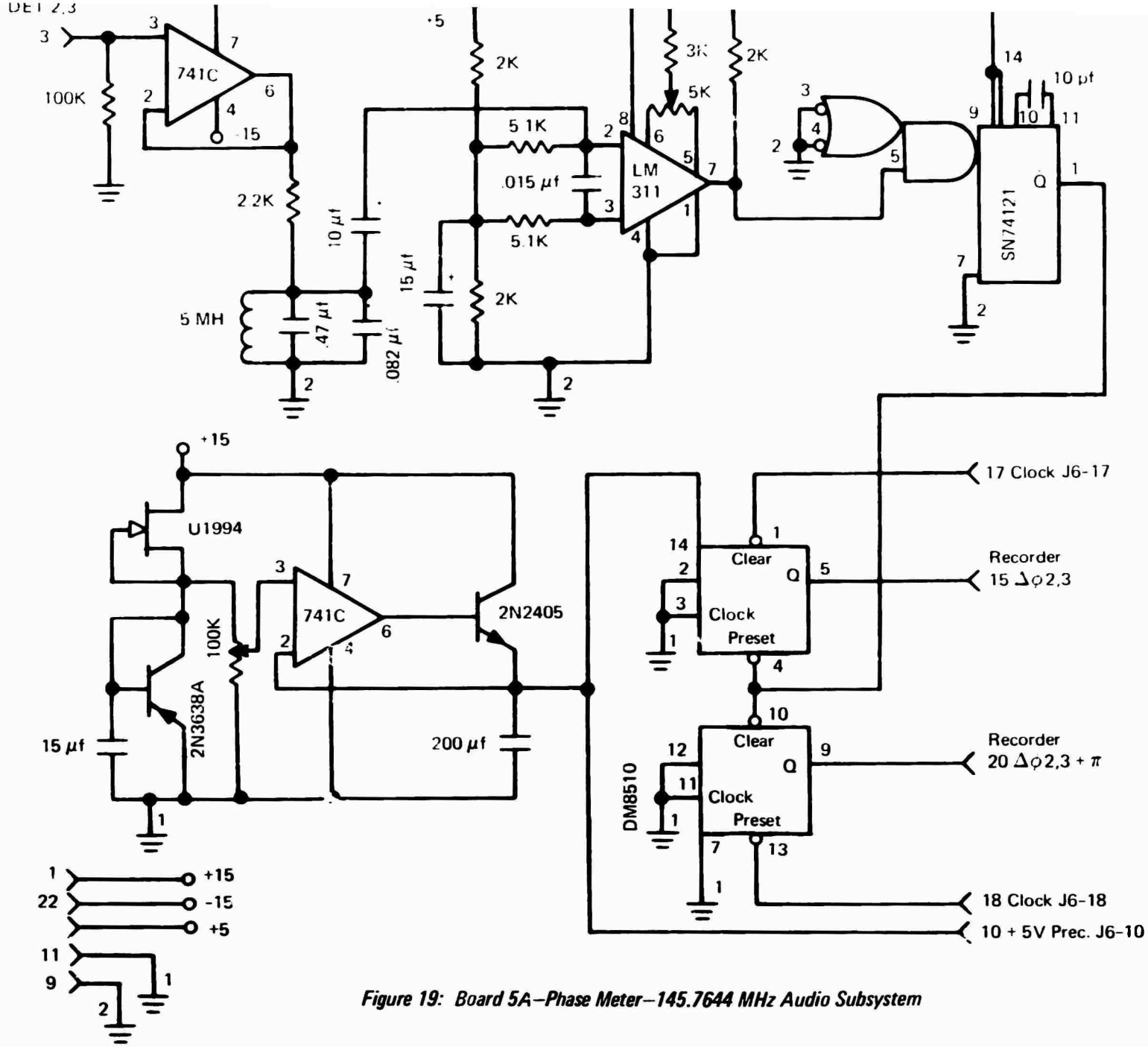

Figure 19: Board 5A—Phase Meter—145.7644 MHz Audio Subsystem

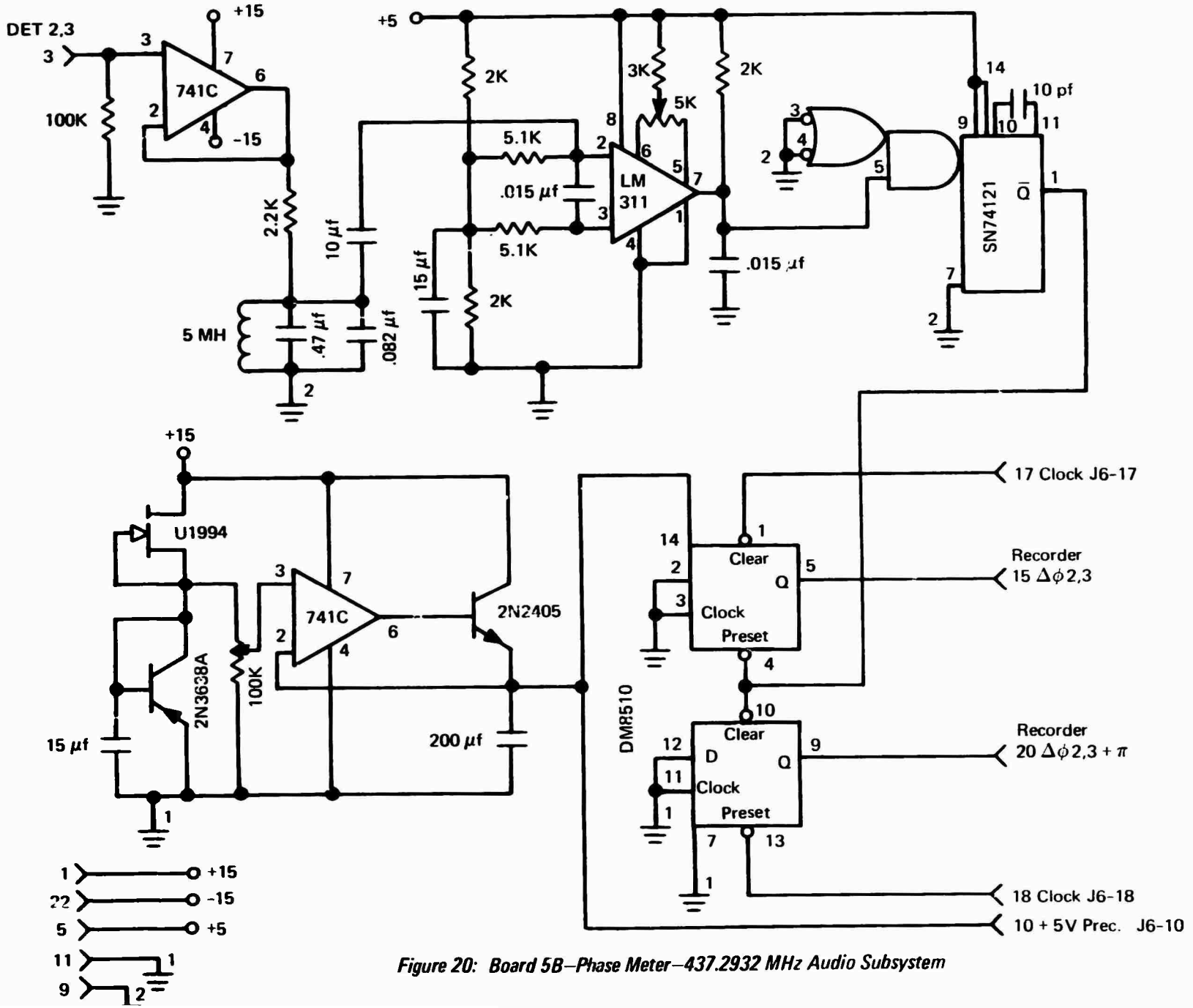

Figure 20: Board 5B—Phase Meter—437.2932 MHz Audio Subsystem

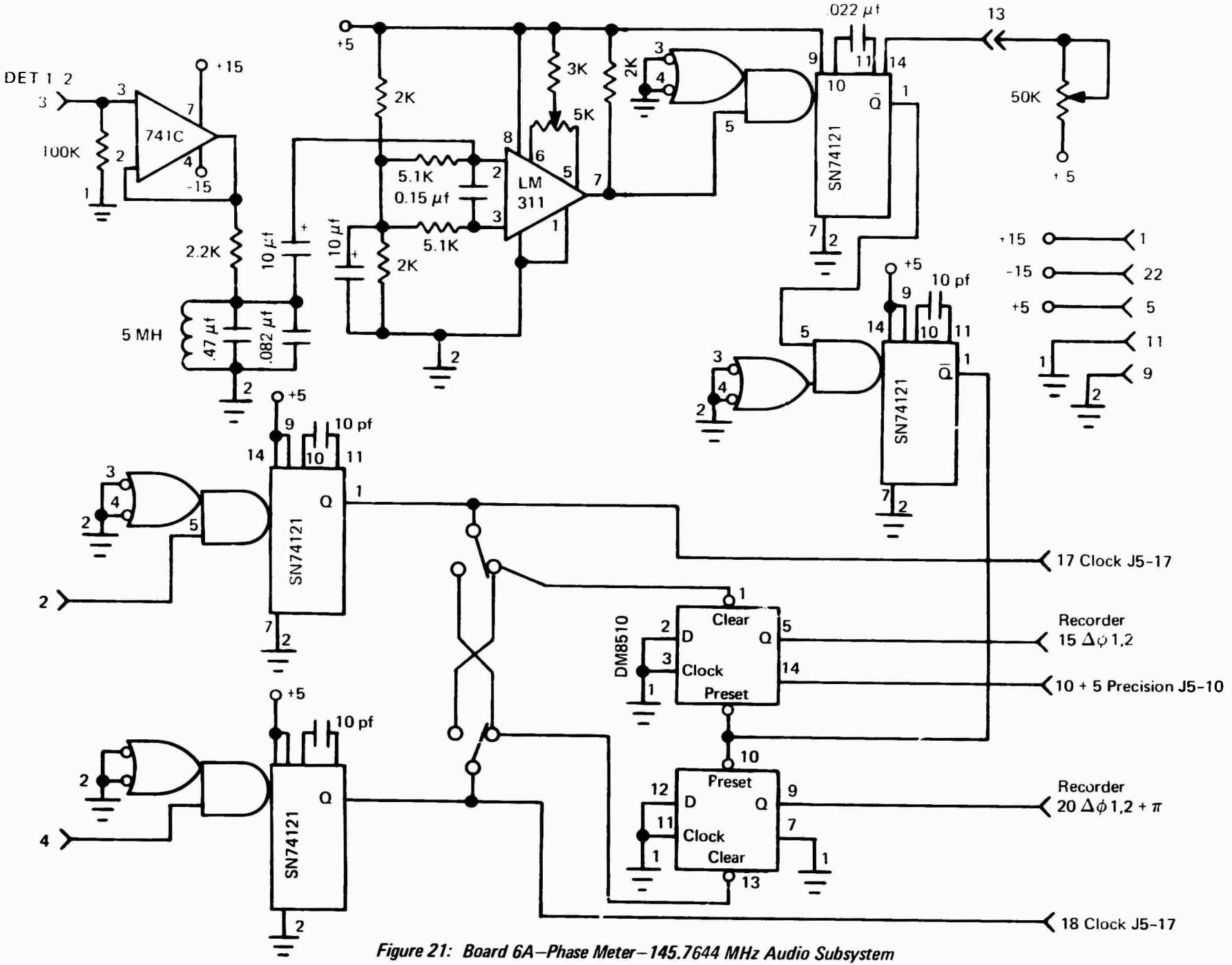

Figure 21: Board 6A—Phase Meter—145.7644 MHz Audio Subsystem

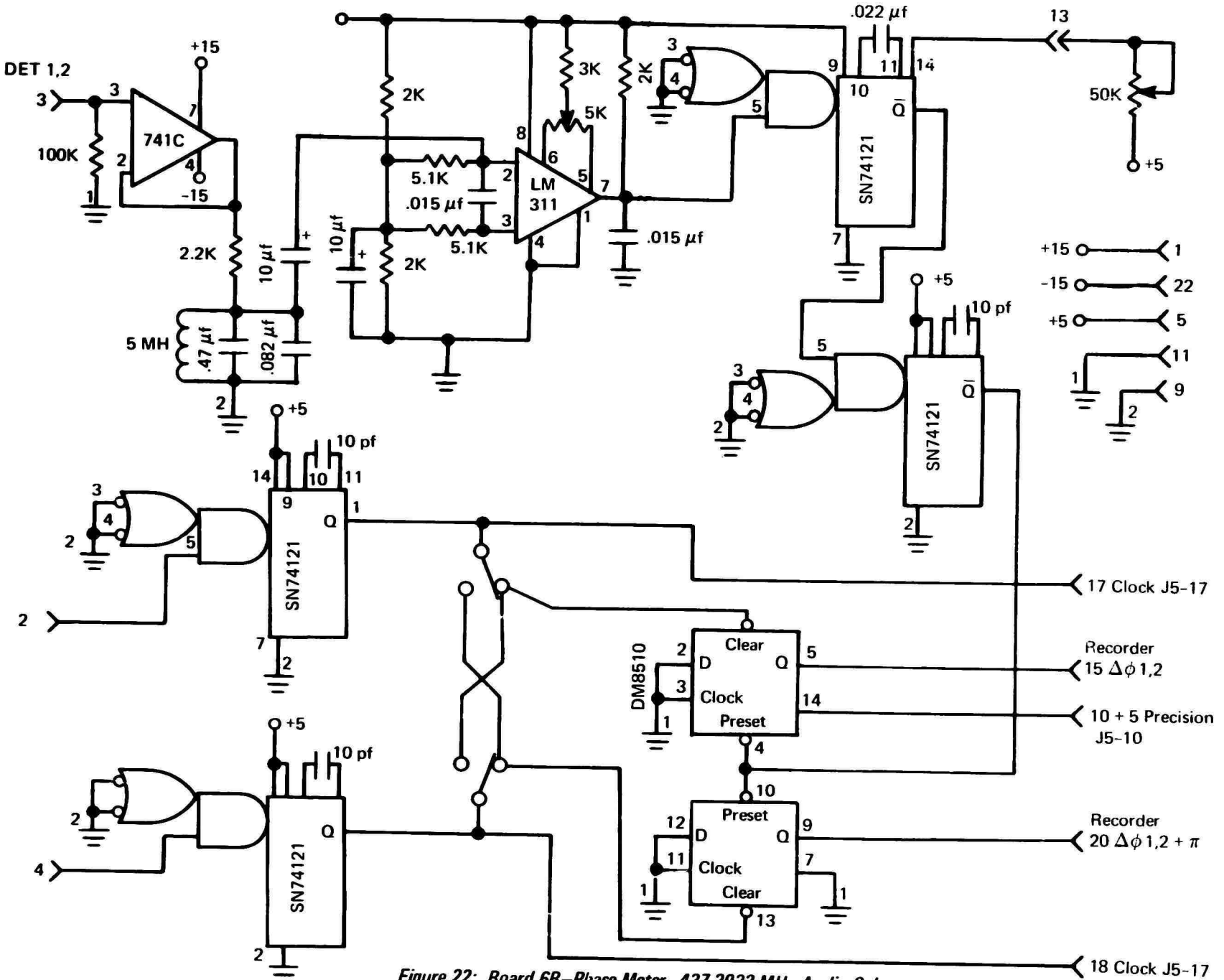

Figure 22: Board 6R—Phase Meter, 427.2933 MHz Audio Out

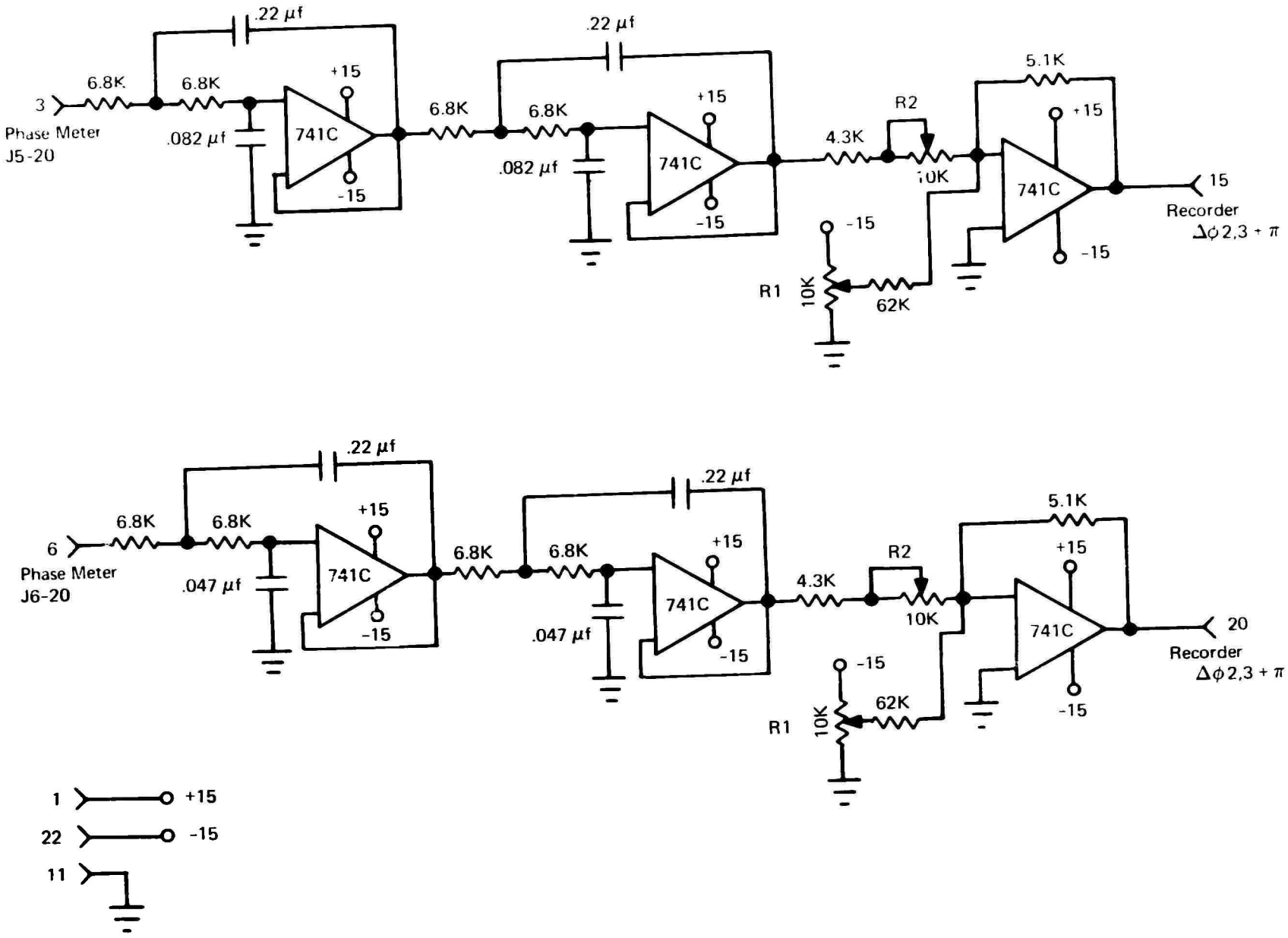

Figure 23: Board 7—Low Pass Filter—145.7644 MHz Audio Subsystem

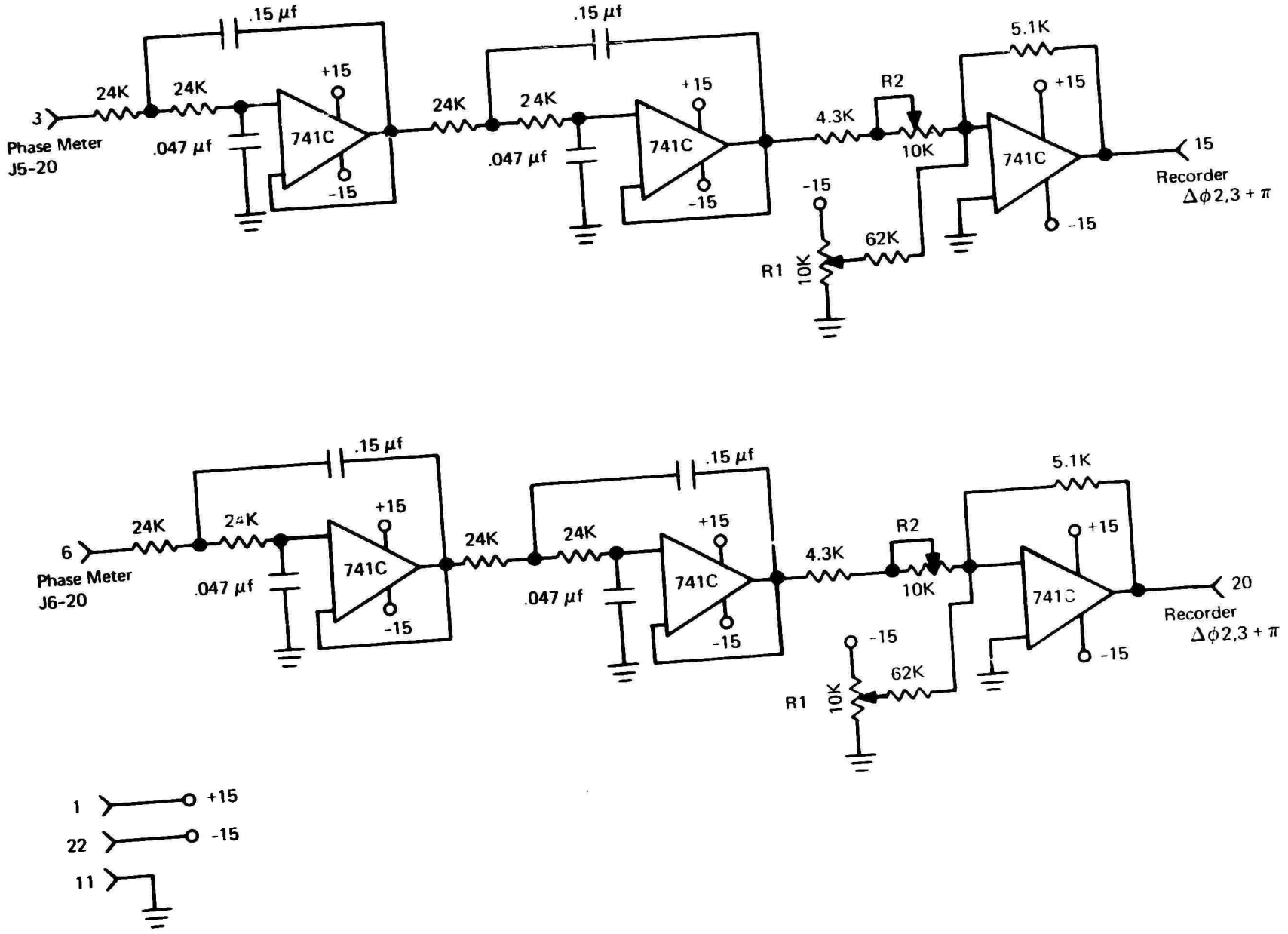

Figure 24: Board 7–Low Pass Filter–437.2932 MHz Audio Subsystem

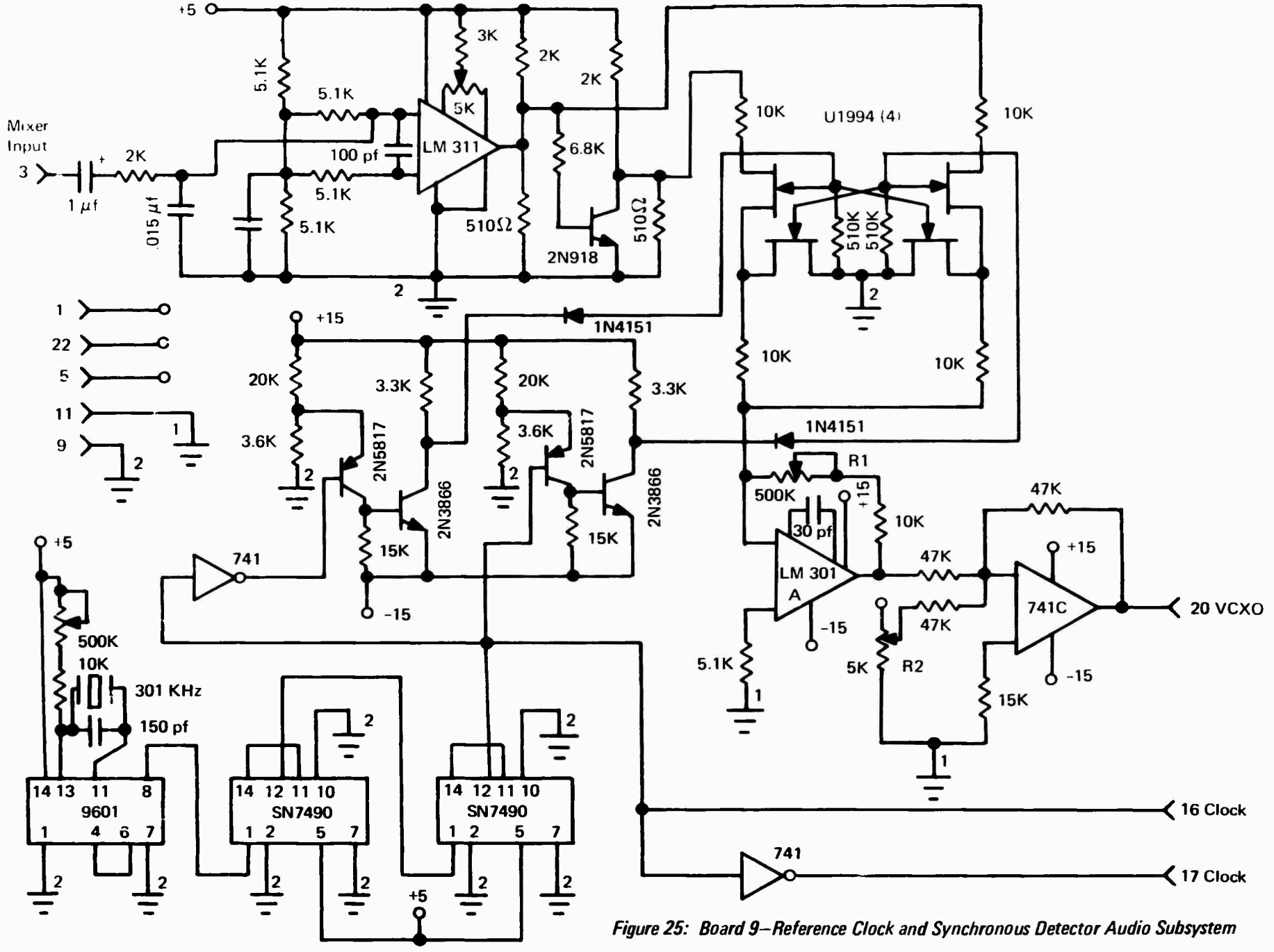

Figure 25: Board 9—Reference Clock and Synchronous Detector Audio Subsystem

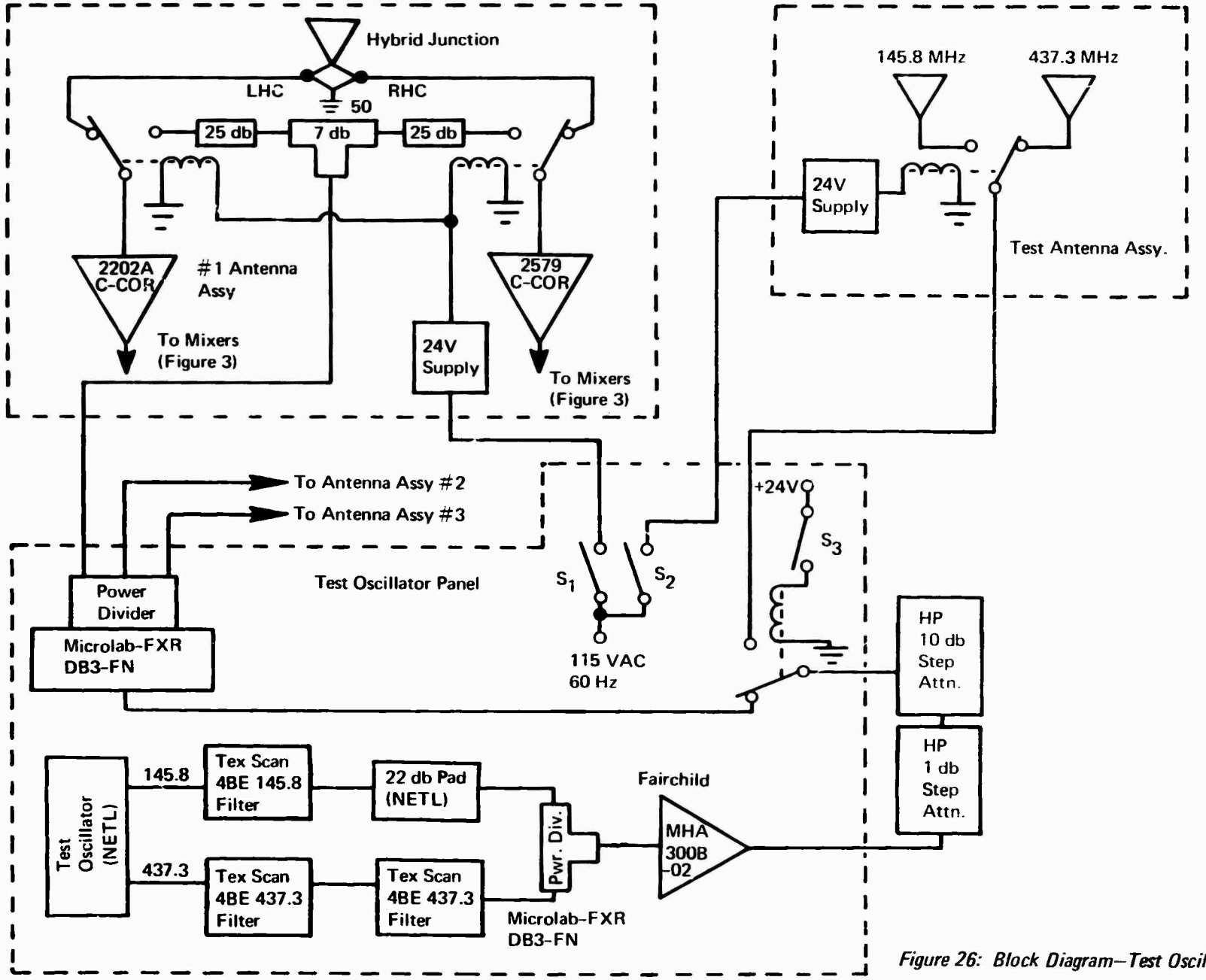

Figure 26: Block Diagram—Test Oscillator System

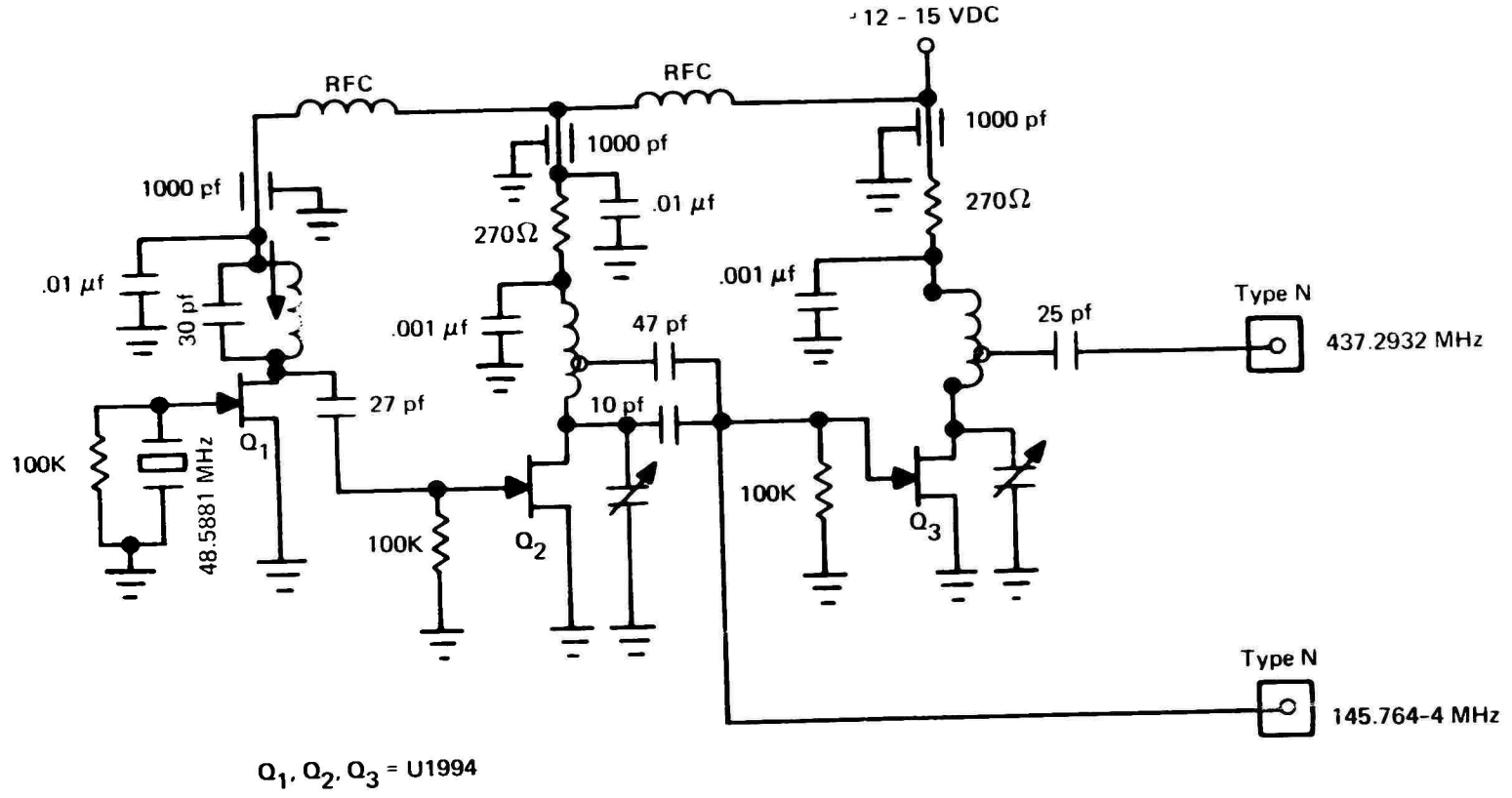

Figure 27: Crystal Test Oscillator Circuit

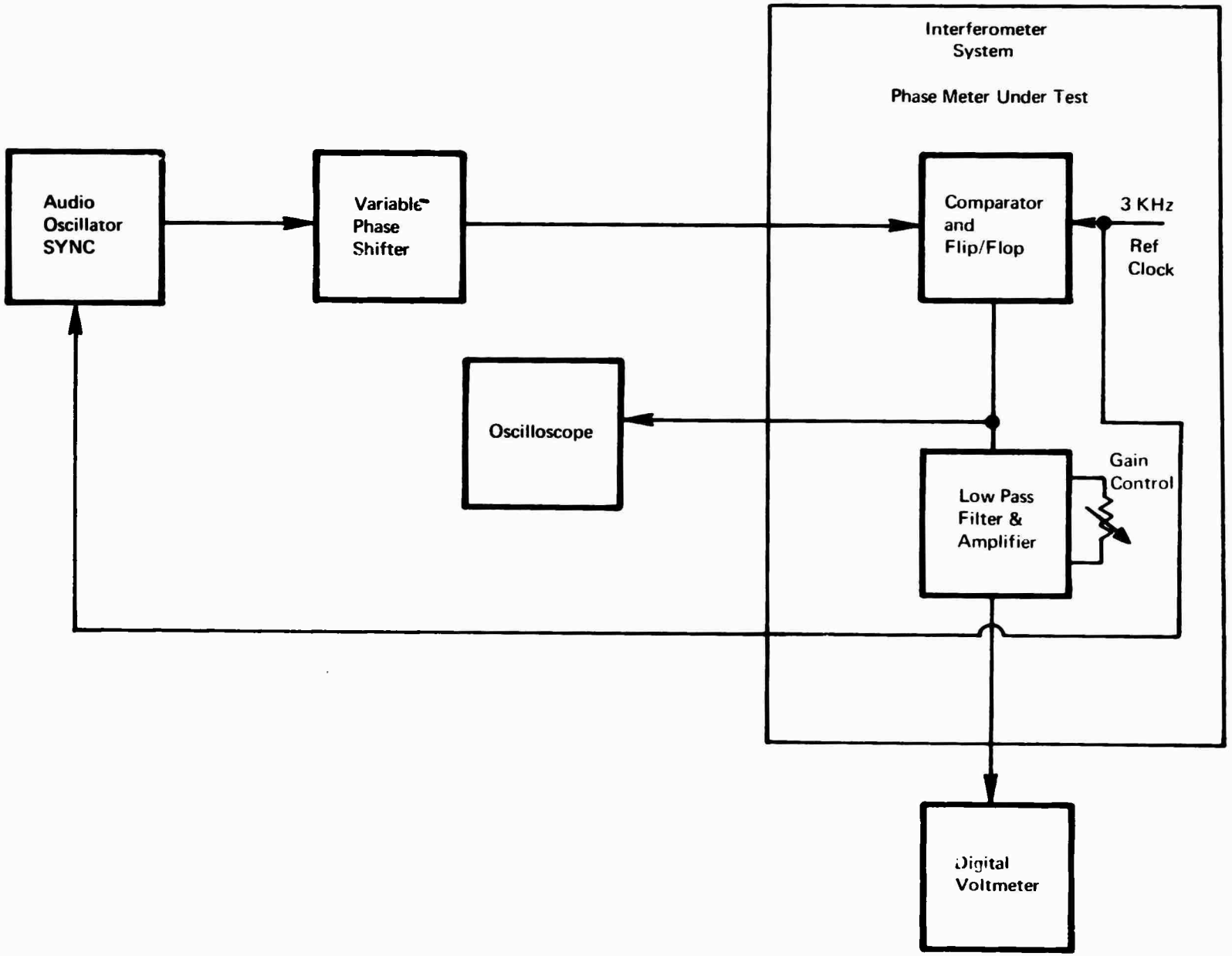

Figure 28: Phase Meter Calibration Test Set-Up

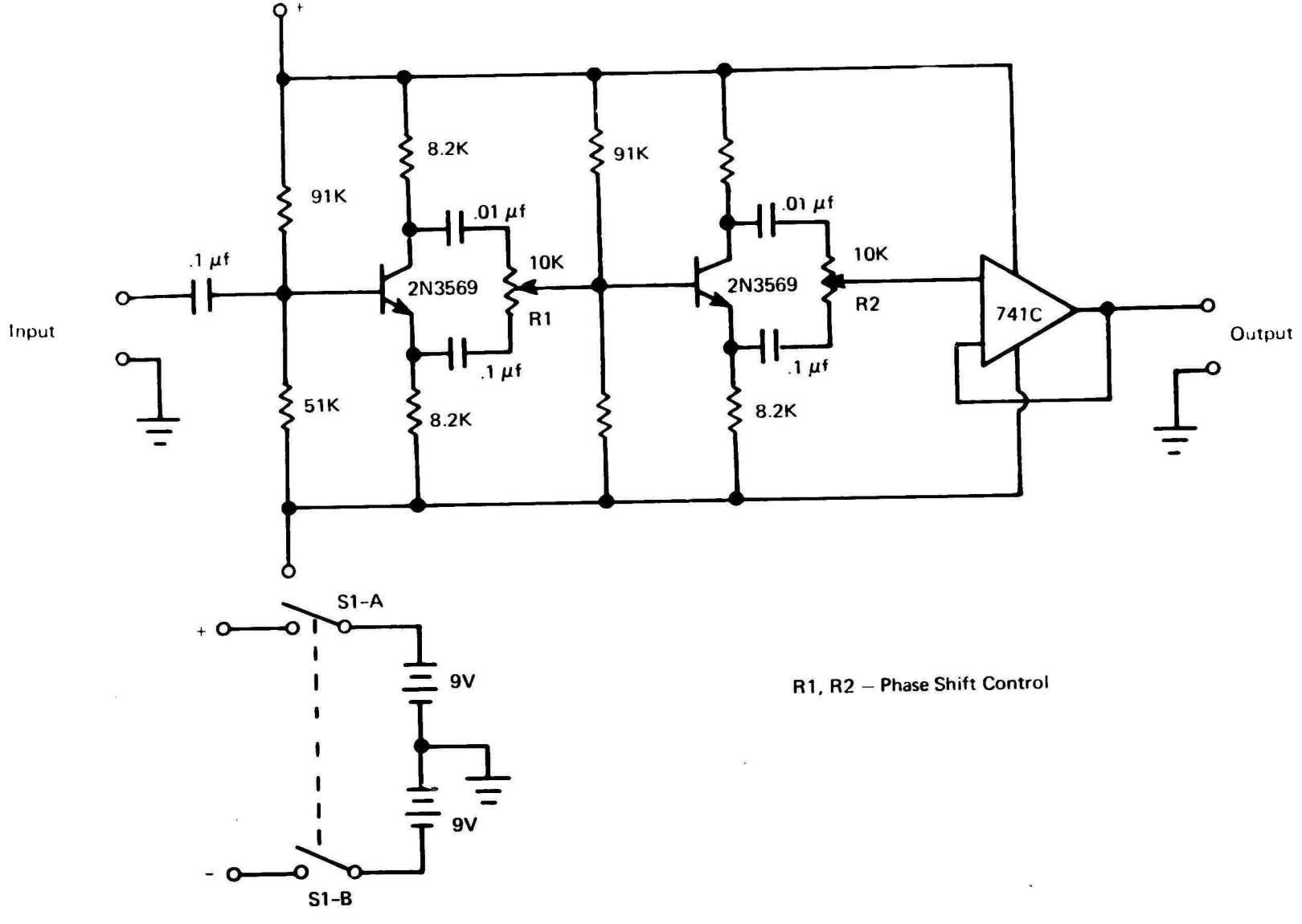

Figure 29: Phase-Shifter Circuit

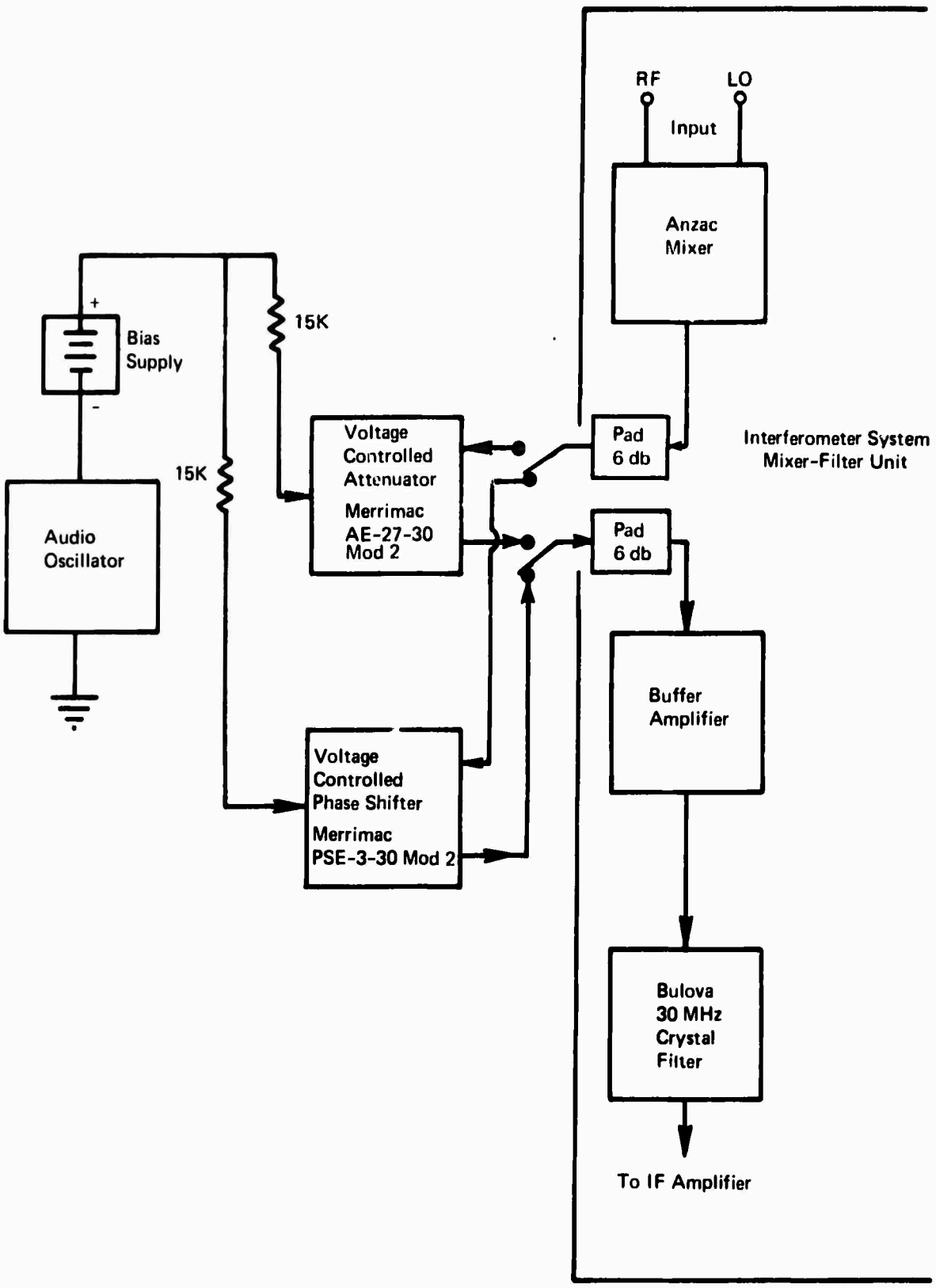

Figure 30: Amplitude and Phase Dynamic Response Test Set-Up

END